Chem Soc Rev

This article was published as part of the

Nanomedicine themed issue

Guest editors Frank Caruso, Taeghwan Hyeon and Vincent Rotello

Please take a look at the issue 7 2012 table of contents to access other reviews in this themed issue

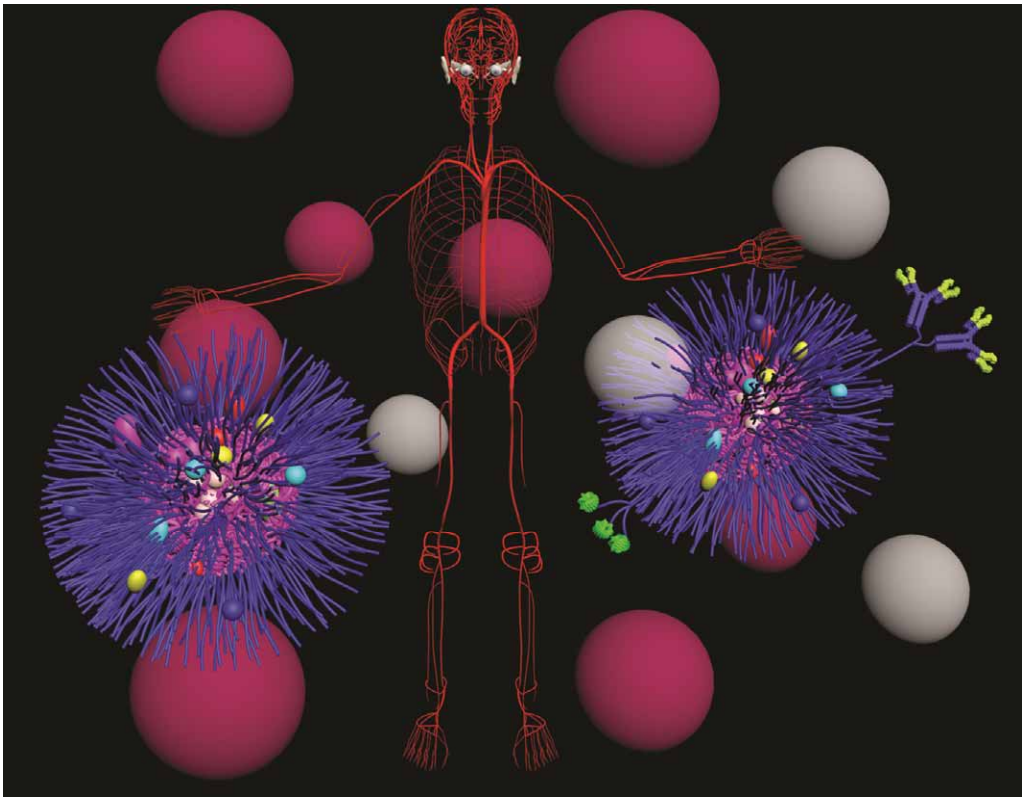

Chem Soc Rev

Dynamic Article Links

Cite this: *Chem. Soc. Rev.*, 2012, **41**, 2780–2799

www.rsc.org/csr

CRITICAL REVIEW

Understanding and controlling the interaction of nanomaterials with proteins in a physiological environment†

Carl D. Walkey[ab] and Warren C. W. Chan*[abcde]

Received 1st September 2011
DOI: 10.1039/c1cs15233e

Nanomaterials hold promise as multifunctional diagnostic and therapeutic agents. However, the effective application of nanomaterials is hampered by limited understanding and control over their interactions with complex biological systems. When a nanomaterial enters a physiological environment, it rapidly adsorbs proteins forming what is known as the protein 'corona'. The protein corona alters the size and interfacial composition of a nanomaterial, giving it a biological identity that is distinct from its synthetic identity. The biological identity determines the physiological response including signalling, kinetics, transport, accumulation, and toxicity. The structure and composition of the protein corona depends on the synthetic identity of the nanomaterial (size, shape, and composition), the nature of the physiological environment (blood, interstitial fluid, cell cytoplasm, *etc.*), and the duration of exposure. In this *critical review*, we discuss the formation of the protein corona, its structure and composition, and its influence on the physiological response. We also present an 'adsorbome' of 125 plasma proteins that are known to associate with nanomaterials. We further describe how the protein corona is related to the synthetic identity of a nanomaterial, and highlight efforts to control protein–nanomaterial interactions. We conclude by discussing gaps in the understanding of protein–nanomaterial interactions along with strategies to fill them (167 references).

Introduction

By virtue of their size, nanomaterials possess enormous design freedom along with the ability to access biological features at the subcellular level. Nanomaterials can combine multiple targeting, sensing, diagnostic, and therapeutic functions and localize to nearly any physiological compartment.[1] For example, a nanomaterial may be engineered to diffuse from blood into a tumor interstitium, recognize and attach to a tumour cell, report its location, internalize in the cell, escape from an endosome, translocate to the nucleus, and release an insoluble cytotoxic drug. This level of functional sophistication is not possible with small molecules, and is a major driver for the development of nanomedicine.

Controlling the interaction of nanomaterials with biological systems is a fundamental challenge of nanomedicine. When a nanomaterial enters a physiological environment, its surface is immediately covered by a layer of proteins, forming what is known as the protein 'corona'.[2] The protein corona alters the size, aggregation state, and interfacial properties of the nanomaterial, giving it a biological identity that is distinct from its synthetic identity. It is the biological identity that determines the physiological response by mediating the interaction of the nanomaterial with biomolecules, membranes, and physical barriers (Fig. 1).[3] Uncontrolled nanomaterial–protein interactions can mark a nanomaterial for uptake in off-target cell populations, activate enzymatic cascades, and prevent efficient removal from the body. A nanomaterial is safe and effective only when its physiological response is understood and controlled.

The interaction of proteins with nanomaterials is an extension of the interaction of proteins with biomaterials. Protein–biomaterial interactions are an integral part of the host response to implants, and have been studied extensively.[4] Many of the principles that govern the interaction of proteins with biomaterials apply to nanomaterials, subject to two caveats. First, the surface of a nanomaterial is highly curved relative to a protein. Second, biomaterials typically remain at the site of implantation, while nanomaterials distribute throughout the body, encountering a wider range of compartments and cell types. In addition, nanomaterials may be internalized in cells *via* endocytosis, gaining access to the intracellular environment.

[a] *Institute of Biomaterials and Biomedical Engineering, University of Toronto, Toronto, ON, M5S 3G9, Canada*
[b] *Donnelly Centre for Cellular and Biomolecular Research, University of Toronto, Toronto, ON, M5S 3G9, Canada*
[c] *Department of Chemical Engineering, University of Toronto, Toronto, ON, M5S 3G9, Canada*
[d] *Department of Chemistry, University of Toronto, Toronto, ON, M5S 3G9, Canada*
[e] *Department of Materials Science and Engineering, University of Toronto, Toronto, ON, M5S 3G9, Canada. E-mail: warren.chan@utoronto.ca*
† Part of the nanomedicine themed issue.

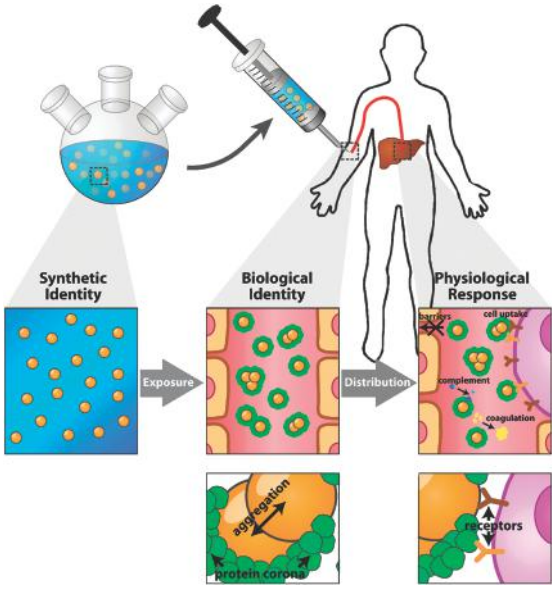

Fig. 1 Relationship between synthetic identity, biological identity, and physiological response. Synthetic identity is the size, shape, and surface chemistry of a nanomaterial post-synthesis. Biological identity is the size and aggregation state of the nanomaterial in a physiological environment, along with the structure and composition of the protein corona. Physiological response is the subsequent interaction of nanomaterials with biomolecules, biological barriers, and cells in the body.

The biological identity of a nanomaterial is a function of its synthetic identity (size, shape, and surface chemistry post-synthesis), the physiological environment, and the duration of exposure. Each physiological compartment has its own distinct set of proteins that interact in a unique way with the nanomaterial. Blood is often the first physiological environment a nanomaterial 'sees' after intravenous administration. Plasma, the acellular portion of blood, contains over 1000 proteins spanning over 10 orders of magnitude in relative abundance.[5] Each of these proteins can potentially interact with a nanomaterial to control its access to specific compartments, mark it for efficient removal by tissue-resident macrophages, and promote undesirable inflammation, thrombosis, and anaphylaxis.[6] As a nanomaterial migrates from blood to other physiological compartments, such as the cell cytoplasm, its biological identity can evolve.[7]

Understanding the biological identity of a nanomaterial and how it determines the physiological response will enable the development of safe and effective nanomedicines. In this review, we discuss the formation, structure, and composition of the protein corona, the techniques used to examine it, how the protein corona depends on the synthetic identity of a nanomaterial, and how it influences the physiological response. We conclude by highlighting strategies to control protein adsorption in order to achieve a desired physiological response, and offer perspective on future developments in this area.

Techniques to study protein corona composition and structure

The composition and structure of the protein corona is characterized by five parameters: (1) thickness and density, (2) identity and quantity, (3) arrangement and orientation, (4) conformation, and (5) affinity. Together, these parameters define the interaction of a nanomaterial with a physiological environment. The thickness and density of the protein corona determines the overall size of the nanomaterial and exposure of the underlying surface. The identity and quantity of the adsorbed proteins determines the array of possible biological interactions along with their strengths. Arrangement and orientation determines the accessibility of potential binding and catalytic domains. Conformation influences the activity of a protein and its interaction with other biomolecules.

Carl D. Walkey

Carl Walkey received his BEng from Carleton University in 2007. He is currently a PhD candidate at the Institute of Biomaterials and Biomedical Engineering at the University of Toronto, studying under Dr Warren Chan. He is supported by an Alexander Graham Bell Canada Graduate Scholarship from the Natural Sciences and Engineering Research Council of Canada (NSERC). His research is focussed on tailoring the nano-bio interface to optimize the performance of nanomaterials for diagnostic and therapeutic applications.

Warren C. W. Chan

Dr Chan is currently an Associate Professor in the Institute of Biomaterials and Biomedical Engineering at the University of Toronto. He also holds the Canadian Research Chair in Bionanotechnology and is affiliated with the Department of Materials Science and Engineering, the Terrence Donnelly Center for Cellular and Biomolecular Research Chemistry, Chemistry and Chemical Engineering. His research interest is in the development of nano- and microtechnology for cancer and infectious disease diagnosis. He has received the BF Goodrich Young Inventors Award, Lord Rank Prize Fund award in Optoelectronics (England), and Dennis Gabor Award (Hungary). Dr Chan received his BS degree from the University of Illinois in 1996 and PhD degree from Indiana University in 2001. He did his post-doctoral training at the University of California (San Diego).

The affinity of a protein to the nanomaterial dictates whether it adsorbs, remains bound, or dissociates during biophysical interactions or translocation to a new physiological compartment.

Techniques to study the composition and structure of the protein corona can be broadly divided into either *in situ* or *ex situ*. *In situ* techniques measure the protein corona while the nanomaterial is dispersed in a physiological environment. These techniques are most relevant, but are limited in number and typically provide the least amount of information. Most measurements are performed *ex situ*, and require isolation of the nanomaterial with its bound protein from the physiological environment. Isolation is typically performed using either differential centrifugation (DC) or size exclusion chromatography (SEC).[8] DC and SEC exploit differences in the size and/or density of a nanomaterial relative to unbound protein. Isolation of the nanomaterial will inevitably disturb the composition of the protein corona, resulting in the loss of weakly bound proteins. The loss of weakly-adsorbed proteins biases subsequent analysis towards strongly-adsorbed proteins. DC subjects the nanomaterials to high centrifugal forces, and is generally thought to perturb the composition of the protein corona more than SEC. Nonetheless, because of its simplicity and availability, DC tends to be more widely applied.

There are a number of techniques that are routinely applied to analyze each parameter of the protein corona. The thickness of the protein corona can be measured using dynamic light scattering (DLS),[9] differential centrifugal sedimentation (DCS),[9] and SEC.[8] DLS is particularly useful as measurements can be made *in situ*. Transmission electron microscopy (TEM) has been applied to study the thickness of the protein corona, but requires counter-staining.[9] Colorimetric protein assays measure the density of the adsorbed protein layer.[10] The strength of protein interactions can be assessed using SEC,[8] isothermal titration calorimetry (ITC),[11] or surface plasmon resonance (SPR).[8] ITC provides additional information on the thermodynamics of protein adsorption, while SPR provides information on adsorption kinetics. Adsorbed protein conformation is measured using circular dichroism (CD)[12] or tryptophan fluorescence quenching.[13] A summary of these techniques along with the corona parameters they measure is provided in Table 1.

Identification and quantification of individual proteins within the corona is generally performed after isolation of the adsorbed protein from the nanomaterial surface. Isolation is performed by treating the nanomaterial with high temperatures, high salt concentrations, detergents, and enzymes. Depending on the strength of the interaction between the protein and the nanomaterial, isolation may be full or partial and can bias subsequent analysis. Following isolation, poly(acrylamide) gel electrophoresis (PAGE) is typically used to fractionate the protein mixture followed by band excision and mass spectrometry,[14] N-terminal protein sequencing,[15] comparison to known gel maps,[16] and densitometry[17] for identification and relative quantification. PAGE is attractive because it is widely available, affordable, and relatively simple. However, it suffers from low throughput, user-bias, lack of sensitivity, and a propensity to form artefacts. More recently, liquid chromatography tandem mass spectrometry (LC-MS/MS) is being applied for simultaneous identification and quantification of the protein corona.[18] LC-MS/MS has higher throughput, greater accuracy, and more sensitivity than PAGE, and introduces less user bias.

Most studies apply *in vitro* models of a physiological environment. For example, isolated plasma and serum are often used as models for blood protein adsorption. However, neither fully represents the *in vivo* environment. Plasma is enzymatically inactive and serum is depleted of coagulation factors. The composition and structure of the protein corona on some nanomaterials is different, depending on whether they are incubated in isolated serum or plasma, or collected after *in vivo* administration.[19,20] Nanomaterials incubated in plasma typically adsorb more fibrinogen, while those incubated in serum adsorb more complement factors.[21]

The current 'toolkit' of techniques to analyze the composition and structure of the protein corona has some drawbacks. First, many techniques measure an ensemble average of all adsorbed proteins, and cannot distinguish individual proteins within the corona. Such techniques are best suited to study the interaction of nanomaterials with individual purified proteins.[11] Second, most measurements are performed *ex situ,* and do not accurately reflect the protein corona *in vivo*. Third, while techniques to study the composition of the protein corona are well-developed, a few techniques are capable of providing information on the structure of the protein corona. Developing new experimental strategies to study the protein corona with structural detail, molecular resolution, and within a physiological environment is an active area of research.[22]

In silico simulation of protein–nanomaterial interactions is gaining popularity as a complement to experimental techniques. Simulation was popularized as a strategy to predict protein folding and protein–protein interactions, but has been successfully adapted to study the adsorption of proteins to biomaterials, and more recently to nanomaterials. Simulation provides

Table 1 Techniques to examine the structure and composition of the protein corona

Corona parameter	Techniques	References
Thickness	Dynamic light scattering (DLS), differential centrifugal sedimentation (DCS), size exclusion chromatography (SEC), transmission electron microscopy (TEM)	8,9
Density	Colorimetric protein assays	10
Identity and quantity	Poly(acrylamide) gel electrophoresis (PAGE), liquid chromatography tandem mass spectrometry (LC-MS/MS)	14–18
Conformation	Circular dichroism (CD), fluorescence quenching, computational simulation	12,13
Affinity	Size exclusion chromatography (SEC), surface plasmon resonance (SPR), isothermal titration calorimetry (ITC)	8,9,11

information on protein orientation and conformation with exceptionally high spatial and temporal resolution, enabling the interaction of a nanomaterial with individual amino acids to be observed over femptosecond timescales.

There are three strategies to simulate protein adsorption: quantum mechanical (QM), all-atom empirical force-field (AA), and coarse-grained (CG).[23] Each is distinguished by the scale of the unit under consideration: QM considers electrons, AA considers atoms, and CG considers groups of atoms. Each strategy offers a trade-off between computational cost and accuracy. QM techniques are highly accurate, but are too computationally demanding for the study of protein adsorption. AA and CG are applied most often, typically as a molecular dynamics (MD) formulation.[24] AA and CG can be combined to produce a 'multiscale' simulation. For example, CG can be used first to determine optimal binding orientations, followed by AA to elucidate the specific interactions between amino acids and the nanomaterial surface.[25]

The quality of the results from a simulation depends on: (1) accurate modeling of the interactions within the system, (2) proper description of water and ions, and (3) sufficient sampling.[24] Simulation results are often erroneous or unrealistic if these factors are not adequately considered. The results of a simulation are generally validated *a posteriori* against experimentally-measured reference values to ensure validity. Detailed discussions on the advantages and disadvantages of different simulation strategies along with the setup of a typical experiment are provided in several reviews.[23,26]

A number of studies have used *in silico* simulation to study protein adsorption to nanomaterials as a function of surface ligand structure,[25] surface curvature,[27] and protein identity.[28] Enzyme activities following adsorption have also been successfully predicted.[29] However, computational power is currently insufficient to handle the complexity of competitive protein adsorption in a physiological environment, and there is a lack of availability of relevant force fields and descriptions of solvation. Techniques and strategies to improve computational efficiency and develop more accurate force fields for nanomaterials is an active area of research.[30] It is likely that *in silico* simulation of nanomaterial–protein interactions will become more widespread as the technique matures.

Mechanisms of protein adsorption

When a nanomaterial enters a physiological environment, it is initially surrounded by high concentrations of free protein. Proteins migrate to the nanomaterial surface either by diffusion, or by traveling down a potential energy gradient. Once in the vicinity of the surface, protein adsorption occurs spontaneously only if it is thermodynamically favourable. In other words, if:

$$\Delta G_{ads} = \Delta H_{ads} - T\Delta S_{ads} < 0,$$

where ΔG_{ads}, ΔH_{ads}, and ΔS_{ads} are the changes in Gibbs free energy, enthalpy, and entropy, respectively, during adsorption, and T is the temperature. There are a number of interactions that contribute to favourable changes in enthalpy ($\Delta H_{ads} < 0$), or entropy ($\Delta S_{ads} > 0$), including the formation of covalent and noncovalent bonds, rearrangement of interfacial water molecules, or conformational changes in either the protein or the nanomaterial surface.[31] The precise mechanisms involved during adsorption and their relative contributions depend on the protein[11] and the physicochemical properties of the nanomaterial.[32]

During adsorption, interactions between the protein and nanomaterial typically occur through a portion of the protein known as a 'domain'. For example, adsorption of high molecular weight kininogen (HMWK) to iron oxide nanoparticles occurs *via* 'domain 5' (D5) of HMWK.[33] D5 is histidine-rich and interacts with iron oxide *via* its imidazole sidechain. Adsorption does not necessarily occur through a single domain, but may instead involve the simultaneous interaction of multiple domains of the same protein with the nanomaterial surface.

The net binding energy of an adsorption event (ΔG_{ads}) determines the stability of the protein–nanomaterial complex. Proteins that adsorb with a large ΔG_{ads} have a low probability of desorption, and tend to stay associated with the nanomaterial.[31] Proteins that adsorb with a small ΔG_{ads} easily desorb and return to solution. Nanomaterials that are charged or hydrophobic tend to form more stable interactions with proteins than those that are hydrophilic.

Proteins may undergo structural rearrangements known as 'conformational changes' during adsorption. Conformational changes are thermodynamically favourable if they allow a hydrophobic or charged sequence within a protein to interact with a hydrophobic or charged nanomaterial surface, respectively.[34] Some amount of conformational change appears to accompany adsorption for the majority of proteins to nanomaterials.[13] However, the degree of conformational change depends on both the chemistry and structure of the protein and the nanomaterial. Proteins with strong internal stabilizing forces (*e.g.* salt bridges or disulfide bonds) usually undergo less severe changes in conformation during adsorption.[35,36]

Charged or hydrophobic nanomaterials alter the conformation of adsorbed proteins more than their hydrophilic counterparts.[37] For example, quantum dots grafted with mercaptoundecanoic acid denature and inactivate the enzyme chymotrypsin, while the same particles grafted with a structurally-similar but hydrophilic poly(ethylene glycol) derivative adsorb the enzyme but do not denature it to the same extent.[38] Similar effects are observed during the adsorption of albumin and fibrinogen to silica nanospheres,[39] or cytochrome *c* to charged gold nanoparticles.[40]

Conformational changes can alter the way in which an adsorbed protein interacts with its environment by exposing sequences that would otherwise be buried in the protein core,[41] or by rearranging a critical binding or catalytic domain.[42] For example, adsorption of β_2-microglobulin to NIPAM/BAM copolymer nanoparticles, quantum dots, carbon nanotubes, and cerium oxide nanoparticles decreases the lag time for protein fibrillation as a result of conformational changes induced upon adsorption.[8] This raises the potential for nanoparticle-induced amyloidosis *in vivo*.

Changes in protein conformation are typically irreversible, even after desorption.[43] For example, conformational changes in the iron-transport protein transferrin are not recovered after desorption from iron oxide nanoparticles.[44] Transferrin is critical for iron transport in the blood, suggesting that nanomaterials may influence physiological function even if they are not directly involved in an interaction.

Protein adsorption does not require direct interaction with the nanomaterial surface, but may occur instead *via* protein–protein

interactions. Protein–protein interactions can be either specific or nonspecific. Specific interactions occur when two or more proteins interact through domains that contain complementary amino acid sequences. For example, protein complexes involving coagulation factors or complement components can assemble on the surface of some biomaterials to mediate the initial humoral response.[45] Nonspecific interactions result from conformational changes that expose charged or hydrophobic domains in a protein which then interact with other proteins. This is a possible mechanism by which α-chymotrypsin forms multilayers on the surface of gold nanorods.[46] Nonspecific protein–protein interactions are not part of the natural biochemistry, and are interpreted as a 'danger signal' by the body, triggering an immune response.[47]

Formation of the protein corona from a complex physiological environment involves the simultaneous adsorption of many proteins by a combination of protein–nanomaterial and protein–protein interactions. Each interaction will have its own characteristic binding energy. As a general observation, proteins within the corona adsorb with either relatively high or relatively low binding energies. Proteins that adsorb with high affinity form what is known as the 'hard' corona, consisting of tightly bound proteins that do not readily desorb, while proteins that adsorb with low affinity form the 'soft' corona, consisting of loosely bound proteins (Fig. 2A).[48] A popular hypothesis is that the hard corona proteins interact directly with the nanomaterial surface, while the soft corona proteins interact with the hard corona *via* weak protein–protein interactions.[9] Alternatively, proteins in the hard and soft coronas may both interact directly with the nanomaterial surface with different binding energies. There is currently little experimental evidence to distinguish between these hypotheses.

Kinetics of protein adsorption

Protein adsorption is a dynamic process, with proteins continually adsorbing to the nanomaterial surface and desorbing from it. Adsorption kinetics refers to the time-dependence of this process. The rates of association and dissociation of a protein to a nanomaterial are described by the parameters k_{on} and k_{off}, respectively. The value of k_{on} depends on the frequency of contact between the protein and the nanomaterial, along with the probability that such a contact results in an adsorption event.[49] Proteins that are present at high concentrations, those that diffuse rapidly, and those that can interact with the nanomaterial surface have large values of k_{on}. The value of k_{off} depends on the binding energy of the protein–nanomaterial complex. Proteins that adsorb with a large binding energy have a lower value of k_{off}. The balance between k_{on} and k_{off} determines the affinity of a protein to the nanomaterial, and is defined by the dissociation constant (K_d).[49] K_d for the adsorption of serum proteins to nanomaterials varies from approximately 10^{-4} M to 10^{-9} M,[11,13,49,50] similar to the range for antibody–antigen interactions. However, as K_d has only been measured for a small subset of proteins and nanomaterials, the actual range of values is probably much higher.

During adsorption from a physiological solution, many proteins compete for binding sites on the nanomaterial surface, each with its own characteristic value of k_{on} and k_{off}. Measuring the k_{on} and k_{off} of each protein in a complex mixture is unfeasible. As an alternative, Cedervall *et al.* modeled total plasma protein adsorption using a biexponential function.[8] This model implicitly divides protein adsorption and desorption into 'fast' and 'slow' components, each with its own 'effective' k_{on} and k_{off}. The fast and slow components of adsorption and desorption presumably represent the hard and soft coronas (Fig. 2A). During plasma protein adsorption to NIPAM/BAM copolymer nanoparticles, the fast component (hard corona) is formed in seconds, while the slow component (soft corona) builds on a timescale of minutes to hours (Fig. 2B). Desorption shows similar behaviour with a mean lifetime of ~10 minutes for the fast component (soft corona), and ~8 hours for the slow component (hard corona) (Fig. 2C).[8] Similar kinetic behaviour applies to plasma protein adsorption to other nanomaterials.[9]

The hard corona is thought to be more important than the soft corona in determining the physiological response to a nanomaterial.[48] As a result of its long residence time, the hard

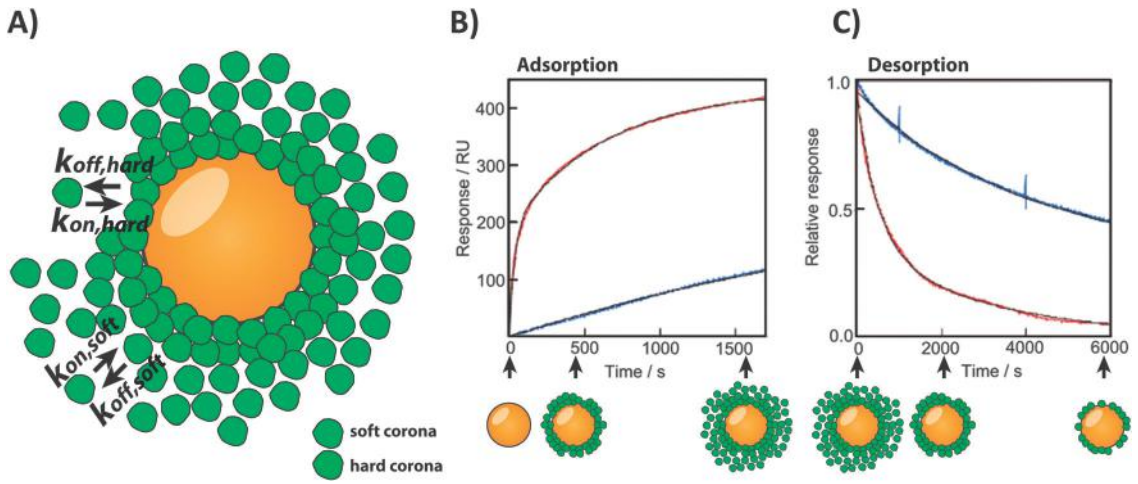

Fig. 2 The protein corona can be subdivided into 'hard' and 'soft' components. (a) Schematic illustrating a conceptualized model for the protein corona. The hard corona consists of strongly-adsorbed proteins at the nanomaterial surface, while the soft corona consists of proteins that associate with the hard corona *via* weak protein–protein interactions. (b) Kinetics of plasma protein association to 50 : 50 (red), and 85 : 15 (blue) NIPAM/BAM copolymer nanoparticles. (c) Kinetics of plasma protein dissociation from NIPAM/BAM copolymer nanoparticles. Figure adapted from Cedervall *et al.*[8] © (2007) National Academy of Sciences, USA.

corona remains adsorbed to a nanomaterial during biophysical events such as endocytosis, and after translocation to a new physiological environment. The soft corona, on the other hand, rapidly dissociates during translocation and is lost. The protein corona reflects the trajectory of a nanomaterial in the body. For example, a nanomaterial that enters the blood through the lung may have a dramatically different protein corona composition and resulting physiological response than the same nanomaterial that is directly injected in the blood.[51]

The rapid initial adsorption of protein from plasma can stabilize a nanomaterial against aggregation. Generally, nanomaterials will aggregate in a solution with high ionic strength as a result of 'charge shielding'. For many nanomaterials, the formation of the hard corona occurs so quickly that it provides a steric stabilizing layer against aggregation by particle contact. For example, citrate-stabilized gold nanoparticles aggregate immediately in phosphate buffered saline (PBS), but are stable in plasma.[52] Protein concentration is a key parameter. At low plasma concentrations, proteins are unable to reach the nanomaterial surface fast enough to prevent aggregation.[53] For example, silica nanoparticles form aggregates in PBS containing plasma at low concentrations, but are well-dispersed in PBS containing plasma at high concentrations.[54] The ability of plasma to stabilize nanomaterials is nanomaterial-dependent. Polystyrene nanoparticles form dimers, trimers, and large aggregates after introduction to plasma, even at high protein concentration.[9,54] This may result from a failure of the protein corona to form sufficiently quickly on these nanoparticles. Alternatively, aggregation may result from the association of nanoparticles with existing protein aggregates, lipoproteins, or microthrombi in plasma,[55] or 'bridging' between proteins on different nanoparticles.[9]

Proteins adsorbed to a nanomaterial are in a continuous state of flux. At any time, a protein may desorb, leaving a surface vacancy that is rapidly filled by another protein of the same or different identity. Changes in the composition of the protein corona resulting from continuous desorption/adsorption are referred to as the 'Vroman Effect'.[56] The Vroman Effect postulates that the identities of the adsorbed proteins can change over time even though the total amount of adsorbed protein remains roughly constant. During the initial formation of the protein corona, proteins with the highest association rates adsorb to a nanomaterial first. If these proteins have short residence times, they will be replaced with other proteins that may have slower association rates, but longer residence times.

During plasma protein adsorption, the Vroman Effect can be divided into 'early' and 'late' stages. The early stage typically involves the rapid adsorption of albumin, IgG, and fibrinogen, which are replaced in seconds by apolipoproteins and coagulation factors.[17,57] Mathematical modeling, and studies using simplified protein mixtures suggest that the high abundance and fast dissociation of albumin and fibrinogen coupled with the low abundance and slow dissociation of apolipoproteins accounts for the sequential adsorption.[58,59] The early stage of the Vroman Effect is not observed for every nanomaterial, implying that some of the proteins that adsorb first may also have long residence times.[60] The late stage of the Vroman Effect occurs as proteins having moderate affinities are replaced by those having very high affinities. A widely-observed example is the increase in adsorbed density of complement component 3 (C3) on polymeric nanoparticles[19] and lipid-coated nanoparticles[61] within minutes and hours following serum exposure. This may result from activation of C3 following contact with the nanomaterial surface. The late stage has been shown to continue for days following exposure of a nanomaterial to plasma,[62] raising the possibility that the protein corona may never reach equilibrium on a biologically-relevant timescale. Depending on which proteins are involved, the evolution of the protein corona with time may have a significant effect on the physiological response to a nanomaterial.

Composition and structure of the protein corona

The identities and quantities of the proteins within the corona play an important role in determining the physiological response to a nanomaterial. Dozens of studies have characterized the identities and quantities of plasma proteins adsorbed to nanomaterials of varying composition. These studies have shown that the protein corona is complex, that there is no one 'universal' plasma protein corona for all nanomaterials, and that the relative densities of the adsorbed proteins do not, in general, correlate with their relative abundances in plasma. Instead, the composition of the protein corona is unique to each nanomaterial, and depends on its synthetic identity.

We compiled a list of identified plasma proteins and their relative abundances for 63 nanomaterials from 26 studies. The purpose was to establish general trends across multiple studies in order to make broad conclusions about the composition of the protein corona. Across all studies, a total of 125 unique plasma proteins were identified, representing the subset of plasma proteins that have been observed to adsorb to at least one nanomaterial. We refer to this subset as the plasma protein 'adsorbome' (Table 2). The physiological function of the proteins in the adsorbome varies, but they are generally involved in lipid transport, blood coagulation, complement activation, pathogen recognition, or ion transport.[63] Although extensive, the list is probably not complete, and will be expanded as more studies are performed in the future on a wider array of nanomaterials.

The plasma protein corona appears to follow a general structure, with 2 to 6 proteins adsorbed at high abundance, and many more adsorbed at low abundance (Fig. 3A). Across all nanomaterials, the most abundant identified protein represents on average 29% of the total adsorbed protein (Fig. 3C), while the top 3 most abundant proteins represent on average 56% (Fig. 3D). The remaining low-abundance proteins account for the balance. While some proteins adsorb abundantly to every nanomaterial, the abundant proteins are not always the same. To illustrate this point, consider the distribution of relative abundances of four example proteins: apolipoprotein AI (Fig. 4A), albumin (Fig. 4B), IgG (Fig. 4C), and fibrinogen (Fig. 4D) across the nanomaterial library. Each of these proteins adsorbs at high abundance on some nanomaterials, but at low abundance on others, depending on the composition of the nanomaterial.

Not every protein within the adsorbome adsorbs at high abundance. Defining a threshold of 10% of the total adsorbed protein mass as 'high abundance', 21 out of 125 proteins have been observed above this threshold on at least one nanomaterial (Table 2—boldface). This observation motivates the division of

Table 2 Summary of the plasma protein 'adsorbome'. The adsorbome consists of 125 plasma proteins that associate with nanomaterials. The adsorbome is compiled from 26 independent studies. Proteins with boldface names adsorb at >10% (relative to total adsorbed protein) on at least one nanomaterial

	Reference																									
Protein	17	154	155	156	157	87	158	67	159	160	147	161	19	74	162	80	163	164	16	165	83	52	166	18	52	167
Actin, cytoplasmic 1																					X		X	X	X	
Alpha 1-antichymotrypsin								X										X							X	
Alpha 2-antiplasmin																							X	X		
Alpha-1-acid glycoprotein 1																X							X			
Alpha-1-antitrypsin	X		X		X				X		X	X			X	X		X			X	X	X			
Alpha-2-macroglobulin											X				X						X		X			
Alpha-actinin-1																					X		X	X		
Angiotensinogen																					X		X			
Ankyrin-1																					X					
Antithrombin-III								X			X		X													
Apolipoprotein (a)																					X		X	X		
Apolipoprotein A-I	X	X	X	X	X	X		X	X	X	X	X	X	X	X	X	X	X	X	X	X		X	X	X	X
Apolipoprotein A-II	X					X			X								X	X		X	X		X			
Apolipoprotein A-IV	X		X	X	X	X			X	X	X	X		X	X		X	X	X	X	X		X			X
Apolipoprotein B-100																					X	X	X	X		
Apolipoprotein C-I																					X		X			
Apolipoprotein C-II	X	X				X			X						X		X	X	X	X	X		X	X		
Apolipoprotein C-III	X		X	X		X		X	X	X		X		X	X		X	X	X	X	X		X	X		X
Apolipoprotein C-IV																					X					
Apolipoprotein D																		X			X		X	X	X	
Apolipoprotein E			X			X			X		X		X		X		X	X	X	X	X		X		X	X
Apolipoprotein F																							X	X		
Apolipoprotein L1																					X		X			
Apolipoprotein M																					X					
ATP synthase subunit																					X		X			
Beta-2-glycoprotein 1			X													X	X					X	X			
Beta-parvin																					X		X			
Cardiotrophin-1											X															
Ceruloplasmin																					X					
Clusterin	X		X	X		X			X	X		X		X	X	X	X	X	X	X	X		X		X	X
Coagulation factor XI																						X				
Coagulation factor XII																						X				
Coagulation factor XIII																					X		X	X		
Complement C1q subcomponent																					X				X	
Complement C1r subcomponent																					X					
Complement C1s subcomponent																					X					
Complement C3			X					X				X	X		X					X	X		X	X	X	
Complement C4																								X	X	
Complement C5																					X		X			
Complement factor B																							X			X
Complement factor H																							X			
Cryocrystalglobulin CC1 kappa light chain																					X					
C-type lectin domain family 4 member F																						X				
Desmoplakin																									X	
Erythrocyte band 7 integral membrane protein																					X		X			
Fermitin family homolog 1																					X					
Fermitin family homolog 3																					X		X			
Fetuin A (alpha 2 HS glycoprotein)									X		X				X						X		X			

Table 2 (*continued*)

Protein	Reference																										
	17	154	155	156	157	87	158	67	159	160	147	161	19	74	162	80	163	164	16	165	83	52	166	18	52	167
Fibrinogen		X	X	X			X	X		X		X	X	X	X		X	X	X	X	X					
Fibronectin																					X					
Filamin-A																					X		X	X		
Galectin-3																					X					
Galectin-3-binding protein																					X					
Gelsolin			X																		X		X	X	X	
Glyceraldehyde-3-phosphate dehydrogenase																					X		X	X		
Haptoglobin	X				X										X	X				X			X			
Haptoglobin-related protein																					X					
Heat shock cognate 71 kDa protein																					X		X			
Hemoglobin										X						X					X		X	X		
Hemopexin											X												X			
Histidine-rich glycoprotein																					X	X	X			
Hornerin																							X		X	
Ig alpha-1 chain C region								X										X					X			
Ig delta chain C region			X					X	X			X			X											
Ig gamma chain	X	X	X		X	X	X	X	X	X	X	X	X	X	X	X		X	X	X							
Ig heavy chain											X															X
Ig kappa chain																					X		X	X		
Ig lambda-1 chain C regions											X										X		X	X		
Ig light chain	X	X	X		X	X	X	X	X		X	X	X	X	X	X		X	X	X							X
Ig mu chain			X		X			X	X			X			X	X			X				X	X		
Ig mu heavy chain disease protein	X																						X			
Integrin																					X		X	X		
Inter alpha trypsin inhibitor H1							X					X									X		X	X		
Inter-alpha-trypsin inhibitor heavy chain H2																					X		X	X		
Inter-alpha-trypsin inhibitor heavy chain H4																					X		X		X	
Kininogen-1																					X	X	X		X	
Leucine-rich alpha-2-glycoprotein																X										
Lipocalin-1																					X					
Lipopolysaccharide-binding protein																					X		X			
Mannan-binding lectin serine protease 1																						X				
Mannan-binding lectin serine protease 2																						X				
Mannose-binding protein C																						X				
Moesin																					X					
Monocyte differentiation antigen CD14																					X					
Multimerin-1																					X		X			
Myosin-9																					X		X			
Myosin-reactive immunoglobulin kappa chain																					X					
Myosin-reactive immunoglobulin light chain																					X					
Paraoxonase-1																					X		X			
Phospholipid transfer protein																						X				
Plasma kallikrein											X											X			X	
Plasma protease C1 inhibitor																					X					
Plasma serine protease inhibitor																					X				X	
Plasminogen																					X					
Platelet glycoprotein Ib alpha chain																					X					
Platelet glycoprotein Ib beta chain																					X			X		

Table 2 (*continued*)

	Reference																										
Protein	17	154	155	156	157	87	158	67	159	160	147	161	19	74	162	80	163	164	16	165	83	52	166	18	52	167
Platelet-activating factor acetylhydrolase																					X					
Pleckstrin																					X		X			
Prenylcysteine oxidase 1																					X					
Properdin																							X			
Proteasome subunit alpha type-1																						X				
Protein AMBP																							X	X		
Proteoglycan-4																						X				
Prothrombin																							X	X		
Pyruvate kinase isozymes M1/M2																					X		X			
Rheumatoid factor C6 light chain																					X					
Serum albumin	X	X	X	X	X	X	X	X	X	X	X	X	X	X	X	X	X	X	X	X	X		X	X	X	X
Serum amyloid A-4 protein																					X		X			
Serum amyloid P component								X																		
Single chain Fv																					X					
Spectrin alpha chain, erythrocyte																					X					
Spectrin beta chain																					X					
Talin-1																					X	X	X	X		
Thrombospondin																					X	X	X	X		
Transcobalamin-2																						X				
Transferrin		X			X					X	X		X								X		X			X
Transthyretin	X								X		X				X					X						
Tubulin alpha-1B chain																					X	X	X	X		
Tubulin beta chain																					X	X	X			
Vinculin																						X	X	X		
Vitamin D-binding protein																					X		X			
Vitamin K-dependent protein S																					X		X	X		
Vitronectin																					X		X	X	X	
von Willebrand factor																					X					
Zymogen granule membrane protein 16																						X				

the blood protein adsorbome into two components: one consisting of blood proteins that can be, but are not necessarily adsorbed at high abundance, and another consisting of blood proteins that are adsorbed only at low abundance. Presumably, the proteins adsorbed at high abundance have the greatest effect on the physiological response *via* enhanced avidity,[64] but this is not necessarily the case.

The total number of unique proteins within the protein corona of any nanomaterial is unknown. Neither PAGE nor LC-MS/MS is sensitive to the single molecule level. Still, LC-MS/MS is more sensitive, and tends to detect more low-abundance proteins. Over the studies considered, PAGE analysis identifies on average 8.9 different proteins per nanomaterial, while LC-MS/MS analysis identifies 67.8 (Fig. 3B). These values can be considered lower bounds on the average number of proteins within the corona. They will undoubtedly be refined as the analysis techniques become more accurate and sensitive.

Broad trends can be identified by comparing results across multiple studies, but care should be taken when comparing protein coronas from individual nanomaterials between different studies. Differences in the blood protein source (serum *vs.* plasma),[19] animal source,[65] protein concentration,[54] diluent,[66] incubation time,[17] purification technique,[8] sample preparation,[67] and analysis technique[33] in each study can influence the identified proteins and their measured abundances. The ratio of plasma to nanomaterial surface area may also be significant, as nanomaterials can deplete low abundance proteins, leading to preferential adsorption of high abundance/low affinity proteins when the nanomaterial surface is in large excess.[54]

The plasma protein corona on most nanomaterials is quite thick. For example, the corona is 21–23 nm thick on 30–50 nm citrate-stabilized gold nanoparticles,[52] 26 nm thick on 50 nm SiO_2 particles,[54] and 35.3 nm thick on 200 nm $PSOSO_3$ nanoparticles.[54] Since most plasma proteins have hydrodynamic diameters in the range of 3–15 nm,[68] the coronas on these nanoparticles are too thick to be composed of only a single layer of adsorbed protein. Instead, the corona probably consists of multiple layers. Little detailed information is available concerning the arrangement and structure of these layers. Simberg *et al*. proposed a model for the protein corona consisting of 'primary binders' that recognize the nanomaterial surface directly, and 'secondary binders' that associate with the primary binders *via* protein–protein interactions.[33] This model followed from the observation that kininogen and kallikrein formed an assembly on the surface of iron oxide nanoparticles. Apolipoproteins may engage in a similar process, having been shown to assemble into lipoproteins on the surface of polymeric nanoparticles.[69] Such a multi-layered structure is significant for the physiological response as the secondary binders may alter the activity of the primary binders or 'mask' them, preventing their interaction with the surrounding environment. It is unclear whether the primary/secondary binding pairs assemble on the nanomaterial surface, or are already assembled in solution and adsorb as a unit.

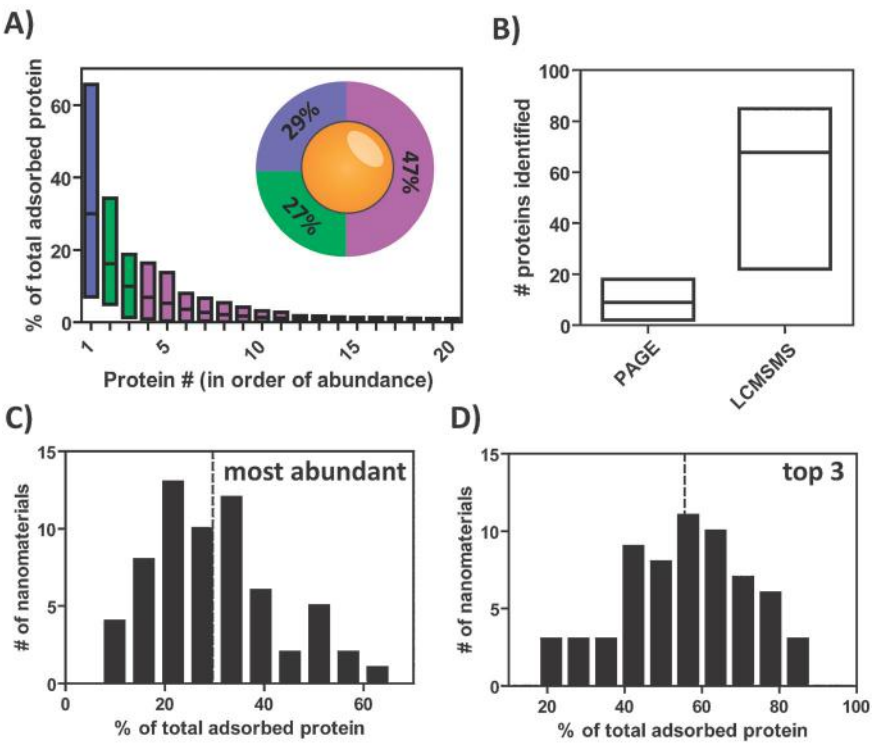

Fig. 3 General model for the protein corona. (a) Adsorbed plasma proteins were compiled from 63 nanomaterials across 26 studies and ordered by abundance. Bars show the average abundance (highest, average, lowest). Inset: Stylisation of an 'average' protein corona. Blue, green, and purple represent the average of the most abundant adsorbed plasma protein, next two most abundant proteins, and remaining adsorbed plasma proteins, respectively. (b) Average number of unique proteins identified using either poly(acrylamide) gel electrophoresis (PAGE) or tandem mass spectrometry (LC-MS/MS). Distribution of % total protein for the (c) most abundant protein, and (d) top 3 most abundant proteins. The dashed line represents the mean of the distribution.

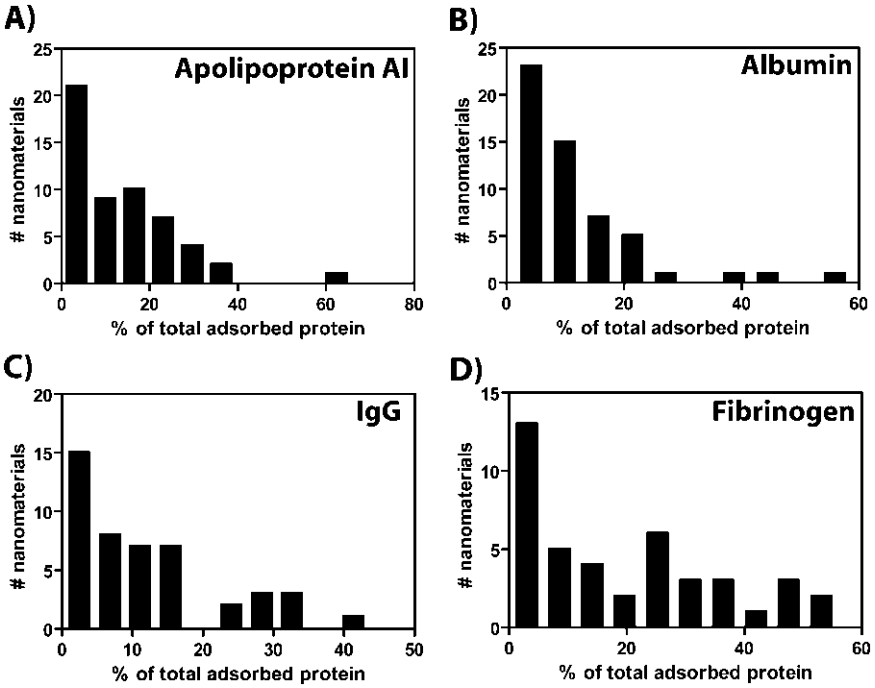

Fig. 4 Distribution of abundances of (a) apolipoprotein A-I, (b) albumin, (c) IgG, and (d) fibrinogen on 63 nanomaterials across 26 independent studies.

Despite its complexity, and variability between nanomaterials, the protein corona tends to give a nanomaterial a zeta potential in the range of −10 mV to −20 mV irrespective of nanomaterial physicochemistry. For example, both anionic and cationic polyelectrolyte-coated gold nanorods have a zeta potential of ∼−20 mV after incubation in serum.[70] Similarly, cationic amine-functionalized polystyrene nanoparticles have a zeta potential of ∼−20 mV after incubation in serum.[71] Serum protein adsorption to gold nanoparticles gives them a zeta potential of ∼−17 mV.[52] The zeta potential does not appear to be strongly size-dependent as 50 nm and 200 nm SiO_2 nanoparticles have zeta potentials of −10.2 mV and −9.6 mV, respectively, after serum exposure.[54] The 'normalization' of zeta potentials is not surprising, given that most plasma proteins carry a net negative charge at physiological pH. In addition, the majority of adsorbed proteins, even across different nanomaterials, tend to have pI < 7.4. A hypothetical nanomaterial may have a positive zeta potential if it preferentially adsorbs plasma proteins with isoelectric points above pH 7.4.

While the composition and structure of the hard corona is becoming increasingly well-characterized, comparatively little is known about the soft corona. Since the soft corona cannot be directly isolated, characterization of its structure and composition is challenging. Most of the studies examining the structure and composition of the soft corona rely on a limited array of *in situ* techniques or apply complex experimental procedures. Cedervall *et al*. examined shifts in the elution times of plasma proteins that were exposed to polymeric nanoparticles using SEC. In theory, proteins that are part of the soft corona will elute earlier than if they were not associated with the nanoparticles. Their analysis implicated 6 serum proteins of varying molecular weight that were presumed to be part of the soft corona. The authors did not identify these proteins explicitly, but did deduce that they were not albumin or IgG.[8] In another study, *in situ* dynamic light scattering was used to show that the thickness of the protein corona on 200 nm $PSOSO_3$ nanoparticles decreased from 50.3 nm to 35.3 nm after washing, suggesting that the soft corona is 15 nm thick on these nanoparticles.[54]

Influence of synthetic identity on the protein corona

In general, any nanomaterial that is exposed to a physiological environment will interact with proteins. However, the extent of these interactions along with the structure and composition of the resulting protein corona depends on the synthetic identity of the nanomaterial. Since protein adsorption occurs at the interface between the nanomaterial and the physiological environment, the chemistry, topography, and curvature of the nanomaterial surface are the most important parameters governing protein interactions.

Nanomaterials with hydrophobic or charged surfaces tend to adsorb more proteins, and denature them to a greater extent than those with neutral and hydrophilic surfaces.[72] For example, increasing the negative charge density and hydrophobicity of polystyrene nanoparticles increases total protein adsorption from plasma.[73,74] Likewise, more hydrophobic NIPAM/BAM copolymer nanoparticles adsorb more protein than their hydrophilic counterparts.[8]

Increased protein adsorption to a nanomaterial results from either higher protein affinity, or the presence of more protein binding sites. For example, hydrophobic NIPAM/BAM nanoparticles adsorb more albumin molecules than hydrophilic NIPAM/BAM nanoparticles, even though the affinity of the protein to both nanoparticle types is roughly the same.[11] This suggests that hydrophobic NIPAM/BAM copolymer nanoparticles

have more protein-binding sites, but the strength of the protein interaction with each binding site is similar. This may result from 'clustering' of the hydrophobic polymer chains, forming distinct 'islands' which act as protein binding sites. In contrast, the affinity of proteins to nanomaterials with uniform surface chemistry tends to increase with increasing charge density and hydrophobicity.[32]

Surface charge and hydrophobicity also correlate with the activation of the complement and coagulation pathways by nanomaterials. For example, liposomes bearing anionic or cationic phospholipid headgroups activate complement more efficiently than those bearing neutral headgroups,[75] while liposomes bearing cationic DOTMA or BisHOP lipids induce more blood clotting.[76] Not all hydrophilic nanomaterials avoid complement activation. Those containing nucleophilic hydroxyl groups are known to be potent activators of the alternative pathway *via* direct activation of complement component 3 (C3).[77] Activation of complement and coagulation may result from the interaction of the initiating enzymes with the nanomaterial surface directly, or with the adsorbed protein corona. Activation of complement and coagulation is important both for opsonization[78] and systemic toxicity as it can lead to severe anaphylaxis or thrombosis.[79]

Nanomaterials with anionic or cationic surfaces tend to preferentially adsorb basic or acidic plasma proteins, respectively. For example, anionic or cationic polystyrene nanoparticles preferentially adsorb plasma proteins with p$I > 5.5$ or p$I < 5.5$, respectively.[80] A similar observation applies to the adsorption of macrophage cytoplasmic proteins to TiO_2 nanoparticles.[51] Interestingly, charge density does not appear to be important as anionic polystyrene nanoparticles with an effective charge density above ~ 3 uC cm^{-2} show no differences in the identities of the adsorbed plasma proteins.[73]

Hydrophobic nanomaterials tend to preferentially adsorb apolipoproteins, while hydrophilic nanomaterials tend to preferentially adsorb albumin, fibrinogen, and IgG.[14,74] This may result from interactions between the lipid binding domains of the apolipoproteins and the hydrophobic surface of the nanomaterial.[81,82] However, the trend does not apply equally to all members of the apolipoprotein family. For example, ApoA-IV, ApoB, ApoC-III, and ApoE adsorb preferentially to hydrophobic cholestorol or atheronal-B quantum dots, while ApoA-I, ApoA-II, and ApoC-I adsorb preferentially to more hydrophilic NH_2-modified quantum dots.[83] Broad classifications of proteins according to physiological function (apolipoproteins in this example) do not account for significant structural variations between them, which appears to be important for their adsorption to surfaces in general and nanomaterials in particular.[84]

Classifying nanomaterials based on charge and hydrophobicity is not sufficient to fully describe the protein corona composition.[85] For example, despite having the same charge sign, polystyrene nanoparticles functionalized with $N(CH_3)_3$ adsorbed more α_1-acid glycoprotein, ApoJ, and ApoA-I, but less IgG and albumin than those functionalized with NH_2. At the same time, polystyrene nanoparticles functionalized with SO_3 groups adsorb more ApoH, but less albumin and IgG than those functionalized with COOH groups.[80] Similarly, despite having nearly identical surface charge densities, ZnO, TiO_2, and SiO_2 nanoparticles each adsorbed different sets of plasma proteins.[86] Comparable observations apply to surfactant-stabilized emulsions,[87] and macroscopic surfaces.[88] In another example, $\sim$90 nm methylstyrene nanoparticles adsorbed significantly more plasma protein than $\sim$90 nm *tert*-butylstyrene nanoparticles, even though they have nearly identical hydrophobicity. Gessner *et al.* speculated that this may be due to increased steric hindrance by the larger *tert*-butyl functional groups.[74] Evidently, the size, structure, chemistry, and arrangement of surface functional groups are important determinants of nanomaterial–protein interactions.

The interaction of proteins with nanomaterials is distinct from the interaction of proteins with bulk materials of the same composition. The highly curved surfaces of nanomaterials increase the deflection angle between adsorbed proteins, decreasing protein–protein interactions.[89] For example, there is substantial cooperativity during the adsorption of histone, γ-globulin, fibrinogen, insulin, and human serum albumin to 100 nm, but not 5 nm gold nanoparticles. In other words, proteins adsorbed to small nanoparticles have little influence on subsequent adsorption events.[13] Less interaction between adjacent adsorbed proteins can lead to higher monolayer densities on smaller nanoparticles. For example, the density of albumin adsorbed to gold nanoparticles increases significantly as the size decreases below 30 nm.[90]

Increasing surface curvature tends to lower the affinity of a protein to the nanomaterial, presumably by decreasing the area of interaction. The dissociation constants of histone, γ-globulin, fibrinogen, insulin, and human serum albumin were approximately 2 orders of magnitude larger (meaning a lower affinity) on 5 nm gold nanoparticles than on 100 nm gold nanoparticles.[13] The affinities of large proteins and protein assemblies appear to be more affected by curvature. For example, 200 nm liposomes consume far less complement from serum than 400 nm and 800 nm liposomes of the same composition.[91] Harashima *et al.* suggested that the decreased activation of complement on $<$200 nm liposomes was due to the inability of the bulky C3 convertase to form on highly curved surfaces.[92] Vertegel *et al.* showed that decreasing curvature enhances the attractive potential between a charged nanomaterial and proteins of opposite charge.[93] This may contribute to the formation of protein multilayers on nanomaterials with low curvature.

Proteins adsorbed to highly curved nanoparticles tend to undergo fewer changes in conformation than those adsorbed to less curved surfaces. Cytochrome *c*, for example, retains a more native-like conformation on 4 nm compared to 15 nm or 35 nm SiO_2 nanoparticles.[94] Similarly, human carbonic anhydrase I is less denatured on 6 nm compared to 9 nm or 15 nm SiO_2 nanoparticles. This may be the result of a larger thermodynamic barrier to protein 'spreading' on more highly curved nanomaterials.[46] Decreased protein–protein interactions may also contribute. For example, increasing the density of lysozyme on 20 nm and 100 nm SiO_2 nanoparticles resulted in greater conformational changes under otherwise identical conditions, but this same trend was not observed on 4 nm SiO_2 nanoparticles.[93] The tendency of smaller nanoparticles to preserve protein conformation seems to be protein-dependent. Fibrinogen, for example, undergoes larger structural changes on smaller rather than larger SiO_2 nanoparticles. Roach *et al.* suggested that this is the result of differences in

Table 3 Qualitative relationships between changes in nanomaterial physicochemical properties during synthesis and the parameters of the resulting protein corona

		Nanomaterial physicochemical property		
		↑ Hydrophobicity	↑ Charge density	↑ Curvature
Corona Parameter	Density/thickness	Increase	Increase	Increase
	Identity/quantity	More apolipoproteins	No change	Not clear
	Conformational change	Increase	Increase	Decrease
	Affinity	Increase	Increase	Decrease

protein orientation and the absence of stabilizing protein–protein interactions.[39]

The influence of surface curvature on the composition of the protein corona is not clear. Some studies have reported qualitative differences in the identities and quantities of adsorbed plasma proteins on nanomaterials of varying size,[52,63] while others have found no observable differences.[14] There has been no comprehensive study of plasma protein adsorption to nanoparticles in the 10–100 nm size range.

Despite a great deal of empirical evidence, a clear relationship between the synthetic identity of a nanomaterial and the structure and composition of the protein corona has not yet emerged. The most important physicochemical parameters appear to be defined, but the sheer complexity of the interactions, along with variable experimental strategies, and partial characterization of the nanomaterials makes concrete relationships elusive. The general empirical trends that have been found are summarized in Table 3.

Influence of biological identity on the physiological response

The biological identity of a nanomaterial (size, aggregation state, and protein corona) determines its interactions with biomolecules and biological barriers in a physiological environment. The outcome of these interactions controls the signalling, kinetics, biodistribution, and toxicity of a nanomaterial *in vivo*. Biological barriers include both 'static' barriers, such as endothelial fenestrae, and 'dynamic' barriers, such as cell membranes.

There is a strong positive correlation between the plasma protein binding capacity of a nanomaterial and the rate at which it is taken up by cells *in vitro*[95] and *in vivo*.[20] Nanomaterials that readily adsorb plasma proteins tend to interact strongly with tissue-resident macrophages of the reticuloendothelial system (RES), leading to rapid blood clearance and accumulation in the liver and spleen. For example, PC : CH (55 : 45) liposomes adsorb ~21 g serum protein per mol lipid, and have a blood half-life of ~120 minutes in mice, while PC : CH : CL (35 : 40 : 10) liposomes adsorb ~101 g serum per mol lipid, and are cleared from circulation almost immediately.[20] Plasma protein binding capacity also correlates positively with cellular cytotoxicity, as a result of stronger cell–nanomaterial interactions.[96]

A subset of plasma proteins called 'opsonins' promote the phagocytosis of nanomaterials by macrophages. Adsorption of the major plasma opsonin IgG enhances the recognition and uptake of a number of nanomaterials by macrophage both *in vitro* and *in vivo*.[97,98] For example, adsorption of IgG to the surface of liposomes enhances their uptake by isolated liver macrophages approximately 6-fold,[99] while crosslinking IgG to the surface of iron-oxide nanoparticles enhances their rate of uptake by macrophages approximately 10-fold both *in vitro* and *in vivo*.[100] Adsorbed IgG facilitates nanoparticle uptake by interacting with Fc receptors (FcR) expressed on the surface of macrophages.[101] For example, the interaction of adsorbed IgG with CD64 (a high affinity IgG Fc receptor) initiates the phagocytosis of carboxy- and amine-functionalized polystyrene nanoparticles by human macrophages *in vitro*.[98]

FcR recognizes the Fc fragment of an adsorbed antibody. Accessibility of the Fc fragment is critical. Antibodies that adsorb to a nanomaterial specifically *via* their Fab fragment tend to present the Fc fragment to the environment. On the other hand, antibodies that adsorb nonspecifically may have their Fc portion blocked by the nanomaterial surface. Both specific and nonspecific adsorption of an antibody is possible, depending on the nanomaterial formulation.[85] Natural antibodies exist against a number of nanomaterial components including phospholipids, polysaccharides, and some polymers.[102]

Adsorbed complement components are also involved in the clearance of nanomaterials by macrophages. Heat treatment of serum (which abolishes its complement activity) eliminates opsonin-dependent deposition of liposomes in the liver.[103] The opsonizing effect of complement seems to depend on the presence of C3. Pretreating serum with an anti-C3 antibody nearly eliminates serum-dependent uptake of liposomes in a perfused liver model.[91] In a physiological environment, complement adsorption to nanomaterials may progress slowly relative to the initial protein adsorption events. For example, the level of C3 on 50 nm lecithin-coated polystyrene nanoparticles increases dramatically several hours following exposure to serum.[61] Complement-dependent uptake of nanomaterials by macrophages occurs *via* interaction of adsorbed complement components with macrophage complement receptors (CR).[92,104] Depending on the complement receptor involved, complement-dependent phagocytosis requires enzymatic degradation of C3[105] and/or macrophage activation.[91] In the absence of these events, nanomaterials may adhere to the surface of macrophages but will not be internalized.

Fibrinogen is also capable of acting as an opsonin as a result of conformational changes in its γ-chain that exposes a binding site for the Mac-1 receptor. This conformational change occurs during fibrinogen adsorption.[106] For example, fibrinogen adsorbed to 5 nm poly(acrylic acid) coated gold nanoparticles is efficiently transported into Mac-1$^+$ THP-1 cells, but not to Mac-1$^-$ HL-60 cells. However, the effect seems to apply only to highly curved nanoparticles, perhaps as a result of steric hindrance of the Mac-1 binding site or differences in fibrinogen conformation on nanoparticles with low surface curvatures.[12]

Other serum proteins have been implicated as opsonins including α_2-HS-glycoprotein, apolipoprotein H, fibronectin, and others.[107,108] However, the role of these opsonins in determining the kinetics and biodistribution of nanomaterials *in vivo* is unclear.

The combined action of multiple opsonins may be involved in the clearance of a nanomaterial. Simberg *et al.* created mouse models that were deficient in mannose binding lectin, IgG, histidine–proline rich glycoprotein, HMWK, fibronectin, vitronectin, fibrinogen, and C3 to assess the role of each in the rapid clearance of iron oxide nanoparticles *in vivo*.[33] A significant enhancement in circulation half-life of the nanoparticles was not observed for any knockout, indicating that none of these opsonins by themselves played a pivotal role in blood clearance. Macrophage may instead recognize multiple opsonins simultaneously, 'compensating' when one uptake pathway is unavailable. However, knockouts in that study did not span all adsorbed proteins, so it also conceivable that an untested low-abundance opsonin is responsible for clearance.

Adsorbed plasma proteins do not act exclusively as opsonins. Preferential adsorption of apolipoproteins is implicated in the ability of certain nanomaterials to cross the blood–brain barrier,[109] or internalize in hepatocytes.[110]

In certain cases, cell uptake can occur in the absence of adsorbed plasma proteins, in a process known as 'serum-independent' uptake. Serum-independent uptake presumably results from direct recognition of the nanomaterial surface by cell-surface receptors. Many receptors recognize molecular 'patterns' that are common to many nanomaterial components. Scavenger receptors, for example, recognize a broad class of polyanions, and may interact with the surface of anionic nanomaterials.[111] Knocking down expression of scavenger receptor A in RAW 264.7 cells significantly lowers the uptake of anionic SiO_2 nanoparticles.[112] At the same time, transfection of COS-7 cells with the scavenger receptor MARCO dramatically enhanced cell association of anionic polystyrene nanoparticles.[113] Association of these nanoparticles was partially suppressed by pre-incubating cells with polyG, which competes for binding sites on scavenger receptors. Another class of receptors, known as 'toll-like' receptors may recognize nanomaterials with hydrophobic surfaces, as part of the body's programmed response to pathogens or malfunctioning cells and proteins.[47]

Serum-independent cell uptake is typically observed *in vitro* using serum-free cell culture. In many cases, addition of serum can dramatically reduce the efficiency of cell uptake. For example, uptake of oxidized silicon microparticles by HUVEC endothelial cells in serum-containing media is substantially lower than serum-free media.[101] In such cases, serum proteins act as 'dysopsonins' since they lower the rate of cell uptake instead of enhancing it.[114] Dysopsonization is probably the result of the adsorbed proteins blocking the interaction of cellular receptors with the nanomaterial surface.[115] As a result, the nature of the dysopsonin effect depends on the nanomaterial and the cell type. Some cells, particularly macrophage, are equipped with surface receptors that interact as efficiently with the adsorbed protein as the nanomaterial surface.[101] For example, cetylmannoside-modified liposomes are cleared efficiently by perfused livers in the absence of serum, but are cleared even more efficiently upon addition of serum. This appears to be the result of the adsorption of complement components, as treatment of the serum with high temperature or an anti-C3 antibody prior to nanomaterial incubation lowers macrophage uptake to below the levels of the bare liposomes.[116] Presumably, liposome-bound cetylmannoside is recognized by mannose receptors in the absence of serum, but promotes complement activation and deposition of C3 by activating the lectin pathway in the presence of serum. In the presence of serum, the nanomaterials are taken up by specific interaction between the protein corona and complement receptors on the macrophage.[117] In this case, serum alters the cell uptake pathway without dramatically altering cell uptake efficiency by changing the interfacial composition of the nanomaterial.[98]

The relevance of direct cellular recognition of a nanomaterial surface *in vivo* is unclear, as nanomaterials will invariably encounter a protein-rich environment. Some area of nanomaterial surface would have to be exposed and accessible to the appropriate receptors. This may be possible, as dextran and iron oxide are both accessible to binding peptides and antibodies after incubation of iron oxide nanoparticles with plasma.[33] However, this may not be significant for cell uptake since the uptake of serum-treated iron oxide nanoparticles by macrophage is not inhibited by dextran or control nanoparticles without adsorbed protein.[118] If areas of 'bare' iron oxide or dextran were accessible for cell interaction, dextran and control nanoparticles should compete for cell-surface receptors and lower the efficiency of cell uptake. Instead, it appears to be the adsorbed serum proteins that are responsible for cell uptake in this case.

By increasing the overall size of a nanomaterial, protein adsorption changes how it interacts with biological barriers. Nanoparticles with hydrodynamic diameters less than $\sim$5.5 nm are cleared from the blood *via* glomerular filtration in the kidney. For example, cysteine-coated $\sim$3 nm quantum dots that resist protein adsorption are cleared rapidly by the kidney after intravenous administration in mice. On the other hand, DHLA and cysteamine-coated quantum dots grow to over 10 nm in diameter after exposure to serum, preventing renal clearance.[68] At the other end of the size spectrum, rigid nanoparticles greater than $\sim$200 nm in size tend to accumulate efficiently in the spleen, presumably *via* filtration in the splenic red pulp. For example, over 40% of the injected dose of 250 nm poloxamer-407 coated polystyrene nanoparticles accumulate in rat spleen within 24 h, while only $\sim$15% of the 150 nm nanoparticles do.[119] Adsorption of plasma proteins may lower the 'effective' size of a nanomaterial that avoids splenic filtration to well below 200 nm. Alternatively, aggregation of nanomaterials in plasma can increase the size of small nanoparticles to beyond 200 nm.[120] Regardless of the mechanism, it is the biological identity of the nanomaterial, not its synthetic identity that is important for determining its interactions with biological barriers.

In summary, cells can recognize nanomaterials in a physiological environment by receptor interaction with the nanomaterial surface or the adsorbed protein corona. The mechanism responsible for uptake of a given nanomaterial remains unclear. Multiple receptors and multiple mechanisms may be involved simultaneously. For example, macrophage uptake may be driven by the combined action of complement receptors and FcR, not

necessarily one or the other.[121] Nanomaterials are well-known to bind to cells *via* multivalent interactions, engaging multiple copies of the same receptor for internalization. It is conceivable that multiple different receptors could contribute to uptake of a nanomaterial with a complex protein corona. For example, knocking out expression of scavenger receptor A decreases uptake of gold nanoparticles, but does not eliminate it, suggesting the simultaneous involvement of multiple different cell-surface receptor types.[122] The array of mechanisms and their relative contributions depends not only on the cell type, but also on the biological identity of a nanomaterial, in particular the composition and structure of the plasma protein corona. The hard corona is probably the most important determinant of these interactions. Even still, the presence of a protein on the nanomaterial surface does not necessarily imply that it will interact with its corresponding cellular receptor. The orientation and conformation is critical.

Eliminating and controlling protein adsorption

Nanomaterials that adsorb plasma proteins in an uncontrolled way are of limited use as nanomedicines. On top of activating the complement and coagulation cascades, they tend to adsorb opsonins and accumulate rapidly in macrophage of the RES. Macrophage uptake lowers imaging sensitivity and therapeutic efficiency by preventing nanomaterials from localizing to a desired target site. In addition, nanomaterial–macrophage interactions may elicit an inflammatory response or compromise macrophage function.[123] Ensuring the safe and effective application of nanomaterials to diagnose and treat diseases requires that they interact in a controlled and selective way with proteins and cells.

One strategy is to suppress or eliminate protein adsorption. This involves 'passivating' the nanomaterial surface by modifying it with charge-neutral, highly hydrophilic 'anti-fouling' polymers.[108] Modifying a nanomaterial surface with an anti-fouling polymer renders protein adsorption thermodynamically unfavourable. Using high molecular-weight polymer chains is particularly attractive as they have high conformational freedom in an aqueous environment. This creates an additional entropic barrier to protein adsorption, as proteins are required to compress the polymer chains in order to reach the nanomaterial surface.[124]

Both organic and inorganic nanomaterials can be modified with anti-fouling polymers. For some nanomaterials, these polymers may be included during synthesis. For example, poly(ethylene glycol) (PEG) can be incorporated into emulsion-based polymeric nanomaterials as part of an amphiphilic diblock copolymer,[125] or fused to the end of phospholipids for inclusion in liposomes.[126] However, most nanomaterials are modified with anti-fouling polymers post-synthetically. This is accomplished either by physical adsorption or by chemical crosslinking to reactive surface functional groups.[6] Crosslinking is preferred, as polymers that are physically adsorbed tend to desorb over time in a physiological environment.

The surface density of anti-fouling polymer chains is the most important parameter determining the interaction of a nanomaterial with proteins. At low densities, the chains are present in a 'mushroom' conformation, and do not create an effective barrier against protein adsorption. However, at high density, the chains are in the 'brush' conformation, and create a large thermodynamic barrier to adsorption. For example, incorporating PEG at 2% w/w eliminates only 10% of total plasma adsorption to PLA copolymer nanoparticles relative to nanoparticles without PEG. However, incorporating PEG at 5% w/w in the same PLA nanoparticles suppresses 70% of total plasma protein adsorption.[127] In general, the adsorption of a protein is efficiently suppressed as the 'footprint' of the polymer chain on the nanomaterial surface approaches the cross sectional area of the protein.[128] For protein adsorption from plasma, an average polymer chain footprint of approximately 2 nm^2 per chain is critical.[129]

PEG or one of its derivatives is used most commonly as an anti-fouling polymer to modify (or 'PEGylate') nanomaterials for *in vivo* applications.[6] PEG is highly hydrophilic, easy to synthesize, relatively immunologically inert, can be cleared renally, and does not appear to be toxic at low doses. It has been applied as a modifier for pharmaceuticals, and is incorporated into several FDA-approved nanomaterials.[130] Grafting nanomaterials with PEG is effective at slowing nonspecific accumulation in cells (including macrophages) both *in vitro* and *in vivo,* allowing nanomaterials to circulate in the blood for extended periods of time. For example, grafting gold nanorods with PEG at high density gives them a blood half-life of nearly 24 h.[131] Long blood residence times enhance the exposure of PEGylated nanomaterials to a target site, which tends to increase accumulation efficiency. The net tumour accumulation of gold nanoparticles in a xenograft mouse model correlates positively with blood half-life.[132] In this case, the long blood half-life of the gold nanoparticles allows a greater fraction of them to diffuse into the tumour microenvironment *via* the enhanced permeability and retention (EPR) effect.[133]

Although it is widely-used and effective at lowering the nonspecific interaction of nanomaterials with proteins and cells, PEG suffers several drawbacks. First, it can be oxidized in a physiological environment either spontaneously or by enzyme action.[134] Second, even at high densities, PEG is not able to completely eliminate protein adsorption and macrophage uptake. This means that there is a fundamental limit to how much PEG can improve blood circulation half-life.[135] Finally, PEGylated nanomaterials can induce the production of antibodies against them. An initial dose of PEGylated nanomaterials may have a long circulation lifetime, but subsequent doses of the same formulation are rapidly cleared. This is known as the 'accelerated blood clearance' phenomenon.[136]

Developing novel anti-fouling polymers is an active research area. Some potential alternatives to PEG include polyoxazolines, dendrons, polysaccharides, polypeptoids, and zwitterionic polymers.[137] Zwitterionic polymers, in particular poly(carboxybetaine methacrylate) (PCBMA), are more chemically stable than PEG and seem to adsorb less protein over both short and long time periods.[138] For example, self-assembled monolayers (SAMs) of oligo(ethylene glycol) on gold substrates adsorb serum proteins at $\sim$1000 pg mm^{-2}, while SAMs of PCBMA reduce serum adsorption to $<$100 pg mm^{-2}.[139] Nanomaterials that have been modified with PCBMA tend to have exceptionally low nonspecific cellular uptake. For example, crosslinked PCBMA/iron oxide nanogels are internalized at almost undetectable levels in HUVEC cells and macrophages.[140] Low nonspecific cellular uptake has also been demonstrated for chemically similar

sulfobetaine coatings on quantum dots.[141] Zwitterionic polymers have the added advantage of being smaller than PEG, resulting in more compact nanomaterial formulations.[142]

There is a drawback to eliminating plasma protein adsorption. In the hypothetical case where complete suppression of protein adsorption is achieved, the nanomaterial will generally lose affinity to its target.[126] The size and shape of a nanomaterial may help it to localize in a target compartment, but this type of targeting is not usually very efficient. For example, PEGylated gold nanoparticles with a blood half-life of over 16 h in mice accumulated to approximately 1% ID g^{-1} in a xenograft tumor compared to well over 10% ID g^{-1} in the liver and spleen at 24 h.[132] Despite having a long blood half-life, PEGylated nanoparticles accumulated more efficiently in off-target organs than the tumour.

In most cases, molecules (such as antibodies and peptides) that recognize a feature of the target are tethered to the anti-fouling polymer layer to increase target affinity. However, RES macrophage may recognize these ligands either directly or by means of opsonins (such as complement components). As a result, even if target site affinity is increased, net accumulation at the target site may not be enhanced since the rate of RES clearance increases as well. This leads to a paradox whereby one cannot simultaneously achieve high target affinity and long blood half-life. Some strategies are being explored to overcome this including 'sheddable' anti-fouling polymer coatings.[143]

An alternative to preventing the adsorption of plasma proteins is to harness them as targeting molecules. One possibility is to purify a protein from plasma and attach it to a nanomaterial *ex vivo*. For example, transferrin can be covalently linked to a nanomaterial to target cells overexpressing transferrin receptors (TfR).[144] TfR is often upregulated on actively proliferating cells, such as those in tumours.[145] *Ex vivo* attachment is reasonably successful for abundant, stable proteins, but is challenging for low abundance, enzymatically active, or unstable proteins. Purification of these proteins is tedious, expensive, and can disrupt the conformation or destroy the activity of the protein. An alternative is to design a nanomaterial that adsorbs the protein selectively *in vivo*.[146] For example, internalization of poly(ethylene glycol)-modified polyhexadecylcyanoacrylate (PEG-PHDCA) nanoparticles in rat brain endothelial cells (RBEC) is nearly three times more efficient than 'bare' PHDCA nanoparticles as a result of selective adsorption of apolipoproteins B100 and E.[147] These apolipoproteins presumably interact with the low-density lipoprotein receptor (LDL-R) on RBEC. Direct adsorption of plasma proteins *in vivo* avoids the purification process and captures the protein in its native form, but requires sophisticated nanomaterial design to avoid nonspecific adsorption. There is also the challenge of discovering a plasma protein that recognizes the target specifically. For example, besides the brain, LDL-R is expressed by liver hepatocytes.

In summary, modifying a nanomaterial with anti-fouling polymers such as PEG is an effective strategy to suppress the adsorption of plasma proteins and the rate of uptake in off-target cell populations. However, it is critical that the nanomaterial is modified with the polymer at high density. Eliminating plasma protein interactions can lower uptake in off-target cell populations, such as macrophage, but tends to also lower the affinity of a nanomaterial to target cells. As an alternative, nanomaterials may be engineered to preferentially adsorb plasma proteins that direct them specifically to the target, provided an appropriate plasma protein exists.

Summary and outlook

The relationship between nanomaterial design, protein interactions, and the physiological response has been studied for over 20 years. Some general principles have emerged. Results compiled over many studies show that a 'typical' plasma protein corona consists of approximately 2–6 proteins adsorbed at high abundance and many more adsorbed at low abundance. Only a small subset of the plasma proteome, known as the plasma 'adsorbome', binds to most nanomaterials (Table 2). In addition, only a fraction of the adsorbome is ever bound to a nanomaterial at high abundance (Table 2—boldface). There is also a crude understanding of how the synthetic identity of a nanomaterial influences the structure and composition of the protein corona. Finally, the mechanisms governing the interaction of nanomaterials with cells have been established, and many of the major plasma proteins involved in cell recognition and uptake have been identified.

Despite substantial progress, detailed relationships between the synthetic identity, biological identity, and physiological response are not clear. It is also unclear whether every protein in the corona influences the physiological response, or only a subset. Without this knowledge as a guide, it is difficult to design nanomaterials to interact with proteins and cells in a controlled way. As a result, most nanomaterials are modified with anti-fouling polymers to suppress protein adsorption altogether. This reduces off-target cell uptake, but also lowers targeting efficiency.

Fundamentally, the challenge of deciphering these detailed relationships is the complexity inherent in the system. The synthetic identity, biological identity, and physiological response are each described by many parameters. Synthetic identity includes the size, shape, and surface chemistry of nanomaterials. Biological identity includes the structure and composition of the protein corona, along with the size and aggregation state of the nanomaterial in a physiological environment. Physiological response includes the signalling, kinetics, distribution, and toxicity of the nanomaterial *in vivo*. In addition, each parameter is highly variable. Nanomaterials can be synthesized in many different shapes and sizes including spheres, rods, triangles, and cubes. The protein corona consists of dozens of proteins with varying identities and quantities. The cells that interact with these particles have many different phenotypes and surface receptor expression levels.

Bringing order to this complexity will require more rapid and accurate techniques to evaluate the biological identity, particularly the composition of the protein corona. Currently, techniques such as PAGE require multiple days for analysis, and not suitable for screening large libraries of nanomaterials. Quantitative, high-resolution shotgun LC-MS/MS has the potential to dramatically reduce the protein corona characterization time. Currently, this technique is applied to study protein expression levels in complex biological samples; however, it can be adapted to study the composition of the protein

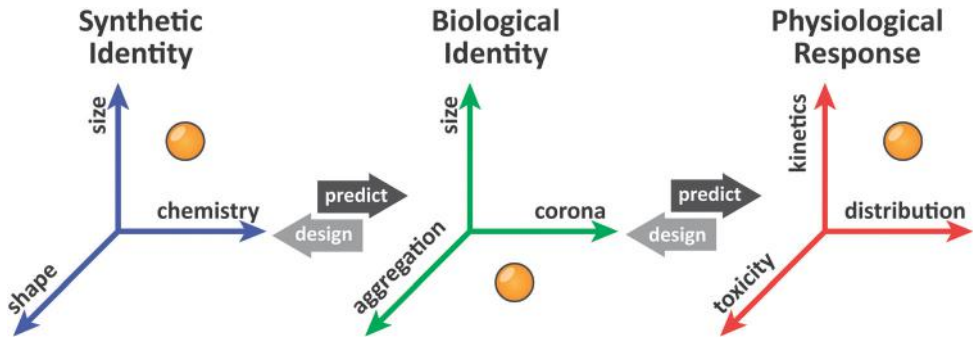

Fig. 5 Schematic showing the relationship between the biological identity and the physiological response. Mapping in the forward direction allows prediction of the physiological response to a novel nanomaterial. Mapping in the reverse direction facilitates rational design of a nanomaterial with a desired physiological response.

corona.[148] This will enable high throughput screening of the protein corona over large libraries of nanomaterials to identify the influence of multiple parameters simultaneously.[149]

The richness of the data sets from high throughput screening will require new analysis strategies. Methodologies can be adapted from systems biology and bioinformatics to group proteins into interaction networks within the protein corona.[150] Much in the same way that a cell stimulus influences the expression of many related genes, varying physicochemical properties of the nanomaterial may influence sets of related adsorbed proteins. Treating changes in adsorbed protein levels in the context of a larger protein interaction network will facilitate the identification of more meaningful relationships.

Techniques are also required to study the structure of the protein corona, specifically the arrangement, orientation and conformation of the proteins within it. The nanomaterial with its adsorbed protein has a similar size and structure to many natural protein assemblies such as viral capsids. Adapting techniques such as cryo-electron microscopy[151] and protein crystallography[152] may be useful for studying the structure and composition of the protein corona but raise significant technical challenges. At the same time, creating sensors using protein tags and site-specific labelling could help determine the structure and orientation of a protein in the corona, and aid in identifying conformational changes. Site directed mutagenesis of specific protein domains will allow the identification of sequences involved in the adsorption of a protein to a nanomaterial.

Once fully mapped, the relationships between synthetic identity, biological identity, and physiological response will enable researchers to predict the physiological response of a nanomaterial by characterizing its synthetic identity (Fig. 5).[153] It will also enable rapid *in vitro* screening of the efficacy and toxicity of new nanomaterials prior to *in vivo* validation. At the same time, these relationships will help guide the rational design of nanomaterials. For example, starting from a required physiological response, parameters of an appropriate synthetic identity may be derived to meet it (Fig. 5). Developing these relationships will require an extensive study. New experimental techniques and strategies will be the major drivers of progress in the future.

Acknowledgements

We would like to acknowledge the Canadian Institute of Health Research, Natural Sciences and Engineering Research Council (NSERC), Canadian Foundation for Innovation, and Ministry of Research and Innovation for funding support. C. W. would like to acknowledge NSERC for graduate fellowship.

References

1 S. M. Moghimi, A. C. Hunter and J. C. Murray, *FASEB J.*, 2005, **19**, 311–330.
2 I. Lynch and K. A. Dawson, *Nano Today*, 2008, **3**, 40–47.
3 A. E. Nel, L. Mädler, D. Velegol, T. Xia, E. M. V. Hoek, P. Somasundaran, F. Klaessig, V. Castranova and M. Thompson, *Nat. Mater.*, 2009, **8**, 543–557.
4 J. M. Anderson, A. Rodriguez and D. T. Chang, *Semin. Immunol.*, 2008, **20**, 86–100.
5 N. L. Anderson, M. Polanski, R. Pieper, T. Gatlin, R. S. Tirumalai, T. P. Conrads, T. D. Veenstra, J. N. Adkins, J. G. Pounds, R. Fagan and A. Lobley, *Mol. Cell. Proteomics*, 2004, **3**, 311–326.
6 N. A. Peppas and D. E. Owens, *Int. J. Pharm.*, 2006, **307**, 93–102.
7 M. Lundqvist, J. Stigler, T. Cedervall, T. Berggard, M. B. Flanagan, I. Lynch, G. Elia and K. Dawson, *ACS Nano*, 2011, **5**(9), 7503–7509.
8 T. Cedervall, I. Lynch, S. Lindman, T. Berggard, E. Thulin, H. Nilsson, K. A. Dawson and S. Linse, *Proc. Natl. Acad. Sci. U. S. A.*, 2007, **104**, 2050–2055.
9 D. Walczyk, F. B. Bombelli, M. P. Monopoli, I. Lynch and K. A. Dawson, *J. Am. Chem. Soc.*, 2010, **132**, 5761–5768.
10 S. K. Sohaebuddin, P. T. Thevenot, D. Baker, J. W. Eaton and L. Tang, *Part. Fibre Toxicol.*, 2010, **7**, 22.
11 S. Lindman, I. Lynch, E. Thulin, H. Nilsson, K. A. Dawson and S. Linse, *Nano Lett.*, 2007, **7**, 914–920.
12 Z. J. Deng, M. T. Liang, M. Monteiro, I. Toth and R. F. Minchin, *Nat. Nanotechnol.*, 2011, **6**, 39–44.
13 S. H. D. Lacerda, J. J. Park, C. Meuse, D. Pristinski, M. L. Becker, A. Karim and J. F. Douglas, *ACS Nano*, 2010, **4**, 365–379.
14 T. Cedervall, I. Lynch, M. Foy, T. Berggad, S. C. Donnelly, G. Cagney, S. Linse and K. A. Dawson, *Angew. Chem., Int. Ed.*, 2007, **46**, 5754–5756.
15 M. Lück, W. Schröder, S. Harnisch, K. Thode, T. Blunk, B. R. Paulke, M. Kresse and R. H. Müller, *Electrophoresis*, 1997, **18**, 2961–2967.
16 T. M. Göppert and R. H. Müller, *J. Drug Targeting*, 2005, **13**, 179–187.
17 T. M. Göppert and R. H. Müller, *Int. J. Pharm.*, 2005, **302**, 172–186.
18 A. L. Capriotti, G. Caracciolo, G. Caruso, C. Cavaliere, D. Pozzi, R. Samperi and A. Laganà, *Anal. Bioanal. Chem.*, 2010, **398**, 2895–2903.
19 E. Allémann, P. Gravel, J. C. Leroux, L. Balant and R. Gurny, *J. Biomed. Mater. Res.*, 1997, **37**, 229–234.
20 A. Chonn, S. C. Semple and P. R. Cullis, *J. Biol. Chem.*, 1992, **267**, 18759–18765.
21 C. Salvador-Morales, E. Flahaut, E. Sim, J. Sloan, M. L. H. Green and R. B. Sim, *Mol. Immunol.*, 2006, **43**, 193–201.

22 L. W. Li, Q. X. Mu, B. Zhang and B. Yan, *Analyst*, 2010, **135**, 1519–1530.
23 A. J. Makarucha, N. Todorova and I. Yarovsky, *Eur. Biophys. J.*, 2011, **40**, 103–115.
24 R. A. Latour, *Biointerphases*, 2008, **3**, FC2–FC12.
25 A. Hung, S. Mwenifumbo, M. Mager, J. J. Kuna, F. Stellacci, I. Yarovsky and M. M. Stevens, *J. Am. Chem. Soc.*, 2011, **133**, 1438–1450.
26 R. Di Felice and S. Corni, *J. Phys. Chem. Lett.*, 2011, **2**, 1510–1519.
27 G. Raffaini and F. Ganazzoli, *J. Appl. Biomater. Biomech.*, 2010, **8**, 135–145.
28 C. Ge, J. Du, L. Zhao, L. Wang, Y. Liu, D. Li, Y. Yang, R. Zhou, Y. Zhao, Z. Chai and C. Chen, *Proc. Natl. Acad. Sci. U. S. A.*, 2011, **108**(41), 16968–16973.
29 G. Zuo, Q. Huang, G. Wei, R. Zhou and H. Fang, *ACS Nano*, 2010, **4**, 7508–7514.
30 F. Iori, R. Di Felice, E. Molinari and S. Corni, *J. Comput. Chem.*, 2009, **30**, 1465–1476.
31 W. Norde, *Pure Appl. Chem.*, 1994, **66**, 491–496.
32 M. De, C. C. You, S. Srivastava and V. M. Rotello, *J. Am. Chem. Soc.*, 2007, **129**, 10747–10753.
33 D. Simberg, J. H. Park, P. P. Karmali, W. M. Zhang, S. Merkulov, K. McCrae, S. N. Bhatia, M. Sailor and E. Ruoslahti, *Biomaterials*, 2009, **30**, 3926–3933.
34 S. Chakraborty, P. Joshi, V. Shanker, Z. A. Ansari, S. P. Singh and P. Chakrabarti, *Langmuir*, 2011, **27**, 7722–7731.
35 T. Verrecchia, P. Huve, D. Bazile, M. Veillard, G. Spenlehauer and P. Couvreur, *6th International Conference on Pharmaceutical Technology*, 1992, **1–5**, 15–25.
36 A. Kondo, F. Murakami and K. Higashitani, *Biotechnol. Bioeng.*, 1992, **40**, 889–894.
37 J. Buijs, C. C. Vera, E. Ayala, E. Steensma, P. Hakansson and S. Oscarsson, *Anal. Chem.*, 1999, **71**, 3219–3225.
38 R. Hong, N. O. Fischer, A. Verma, C. M. Goodman, T. Emrick and V. M. Rotello, *J. Am. Chem. Soc.*, 2004, **126**, 739–743.
39 P. Roach, D. Farrar and C. C. Perry, *J. Am. Chem. Soc.*, 2006, **128**, 3939–3945.
40 M. E. Aubin-Tam and K. Hamad-Schifferli, *Langmuir*, 2005, **21**, 12080–12084.
41 I. Lynch, K. A. Dawson and S. Linse, *Science's STKE*, 2006, **327**, PE14.
42 R. S. Kane and A. D. Stroock, *Biotechnol. Prog.*, 2007, **23**, 316–319.
43 W. Norde and C. E. Giacomelli, *J. Biotechnol.*, 2000, **79**, 259–268.
44 M. M. Mahmoudi, M. A. Shokrgozar, S. Sardari, M. K. Moghadam, H. Vali, S. Laurent and P. Stroeve, *Nanoscale*, 2011, **3**, 3007–1138.
45 J. Andersson, K. N. Ekdahl, R. Larsson, U. R. Nilsson and B. Nilsson, *J. Immunol.*, 2002, **168**, 5786–5791.
46 J. E. Gagner, M. D. Lopez, J. S. Dordick and R. W. Siegel, *Biomaterials*, 2011, **32**, 7241–7252.
47 S. Y. Seong and P. Matzinger, *Nat. Rev. Immunol.*, 2004, **4**, 469–478.
48 I. Lynch, T. Cedervall, M. Lundqvist, C. Cabaleiro-Lago, S. Linse and K. A. Dawson, *Adv. Colloid Interface Sci.*, 2007, **134–135**, 167–174.
49 C. Röcker, M. Pötzl, F. Zhang, W. J. Parak and G. U. Nienhaus, *Nat. Nanotechnol.*, 2009, **4**, 577–580.
50 C. De Roe, P. J. Courtoy and P. Baudhuin, *J. Histochem. Cytochem.*, 1987, **35**, 1191–1198.
51 J. Sund, H. Alenius, M. Vippola, K. Savolainen and A. Puustinen, *ACS Nano*, 2011, **5**, 4300–4309.
52 M. A. Dobrovolskaia, A. K. Patri, J. W. Zheng, J. D. Clogston, N. Ayub, P. Aggarwal, B. W. Neun, J. B. Hall and S. E. McNeil, *Nanomed.: Nanotechnol., Biol. Med.*, 2009, **5**, 106–117.
53 H. T. R. Wiogo, M. Lim, V. Bulmus, J. Yun and R. Amal, *Langmuir*, 2011, **27**, 843–850.
54 M. P. Monopoli, D. Walczyk, A. Campbell, G. Elia, I. Lynch, F. B. Bombelli and K. A. Dawson, *J. Am. Chem. Soc.*, 2011, **133**, 2525–2534.
55 Y. Hong, P. J. Shaw, B. N. Tattam, C. E. Nath, J. W. Earl, K. R. Stephen and A. J. McLachlan, *Eur. J. Clin. Pharmacol.*, 2007, **63**, 165–172.
56 L. Vroman, A. L. Adams, G. C. Fischer and P. C. Munoz, *Blood*, 1980, **55**, 156–159.
57 T. Blunk, M. Lück, A. Calvor, D. F. Hochstrasser, J. C. Sanchez, B. W. Müller and R. H. Müller, *Eur. J. Pharm. Biopharm.*, 1996, **42**, 262–268.
58 D. Dell'Orco, M. Lundqvist, C. Oslakovic, T. Cedervall and S. Linse, *PLoS One*, 2010, **5**, 6.
59 R. J. Green, M. C. Davies, C. J. Roberts and S. J. B. Tendler, *Biomaterials*, 1999, **20**, 385–391.
60 S. Harnisch and R. H. Müller, *Eur. J. Pharm. Biopharm.*, 2000, **49**, 41–46.
61 S. Nagayama, K. Ogawara, Y. Fukuoka, K. Higaki and T. Kimura, *Int. J. Pharm.*, 2007, **342**, 215–221.
62 E. Casals, T. Pfaller, A. Duschl, G. J. Oostingh and V. Puntes, *ACS Nano*, 2010, **4**, 3623–3632.
63 M. Lundqvist, J. Stigler, G. Elia, I. Lynch, T. Cedervall and K. A. Dawson, *Proc. Natl. Acad. Sci. U. S. A.*, 2008, **105**, 14265–14270.
64 W. Jiang, B. Y. S. Kim, J. T. Rutka and W. C. W. Chan, *Nat. Nanotechnol.*, 2008, **3**, 145–150.
65 A. Lesniak, A. Campbell, M. P. Monopoli, I. Lynch, A. Salvati and K. A. Dawson, *Biomaterials*, 2010, **31**, 9511–9518.
66 G. Maiorano, S. Sabella, B. Sorce, V. Brunetti, M. A. Malvindi, R. Cingolani and P. P. Pompa, *ACS Nano*, 2010, **4**, 7481–7491.
67 K. Thode, M. Lück, W. Semmler, R. H. Müller and M. Kresse, *Pharm. Res.*, 1997, **14**, 905–910.
68 H. S. Choi, W. Liu, P. Misra, E. Tanaka, J. P. Zimmer, B. I. Ipe, M. G. Bawendi and J. V. Frangioni, *Nat. Biotechnol.*, 2007, **25**, 1165–1170.
69 E. Hellstrand, I. Lynch, A. Andersson, T. Drakenberg, B. Dahlback, K. A. Dawson, S. Linse and T. Cedervall, *FEBS J.*, 2009, **276**, 3372–3381.
70 A. M. Alkilany, P. K. Nagaria, C. R. Hexel, T. J. Shaw, C. J. Murphy and M. D. Wyatt, *Small*, 2009, **5**, 701–708.
71 G. W. Doorley and C. K. Payne, *Chem. Commun.*, 2011, **47**, 466–468.
72 P. Roach, D. Farrar and C. C. Perry, *J. Am. Chem. Soc.*, 2005, **127**, 8168–8173.
73 A. Gessner, A. Lieske, B. R. Paulke and R. H. Müller, *Eur. J. Pharm. Biopharm.*, 2002, **54**, 165–170.
74 A. Gessner, R. Waicz, A. Lieske, B. R. Paulke, K. Mäder and R. H. Müller, *Int. J. Pharm.*, 2000, **196**, 245–249.
75 D. V. Devine, K. Wong, K. Serrano, A. Chonn and P. R. Cullis, *Biochim. Biophys. Acta, Biomembr.*, 1994, **1191**, 43–51.
76 J. H. Senior, K. R. Trimble and R. Maskiewicz, *Biochim. Biophys. Acta, Biomembr.*, 1991, **1070**, 173–179.
77 L. Liu and H. Elwing, *J. Biomed. Mater. Res.*, 1996, **30**, 535–541.
78 S. T. Reddy, A. J. van der Vlies, E. Simeoni, V. Angeli, G. J. Randolph, C. P. O'Neill, L. K. Lee, M. A. Swartz and J. A. Hubbell, *Nat. Biotechnol.*, 2007, **25**, 1159–1164.
79 J. Szebeni, *Crit. Rev. Ther. Drug Carrier Syst.*, 1998, **15**, 57–88.
80 A. Gessner, A. Lieske, B. R. Paulke and R. H. Müller, *J. Biomed. Mater. Res.*, 2003, **65**, 319–326.
81 A. P. Hitchcock, C. Morin, Y. M. Heng, R. M. Cornelius and J. L. Brash, *J. Biomater. Sci., Polym. Ed.*, 2002, **13**, 919–937.
82 C. Vedhachalam, V. Narayanaswami, N. Neto, T. M. Forte, M. C. Phillips, S. Lund-Katz and J. K. Bielicki, *Biochemistry*, 2007, **46**, 2583–2593.
83 K. Prapainop and P. Wentworth, *Eur. J. Pharm. Biopharm.*, 2011, **77**, 353–359.
84 R. W. Mahley, T. L. Innerarity, S. C. Rall and K. H. Weisgraber, *J. Lipid Res.*, 1984, **25**, 1277–1294.
85 S. C. Semple, A. Chonn and P. R. Cullis, *Adv. Drug Delivery Rev.*, 1998, **32**, 3–17.
86 Z. J. Deng, G. Mortimer, T. Schiller, A. Musumeci, D. Martin and R. F. Minchin, *Nanotechnology*, 2009, **20**, 455101.
87 S. Tamilvanan, S. Schmidt, R. H. Müller and S. Benita, *Eur. J. Pharm. Biopharm.*, 2005, **59**, 1–7.
88 M. Lestelius, B. Liedberg and P. Tengvall, *Langmuir*, 1997, **13**, 5900–5908.
89 H. D. Hill, J. E. Millstone, M. J. Banholzer and C. A. Mirkin, *ACS Nano*, 2009, **3**, 418–424.
90 D. H. Tsai, F. W. DelRio, A. M. Keene, K. M. Tyner, R. I. MacCuspie, T. J. Cho, M. R. Zachariah and V. A. Hackley, *Langmuir*, 2011, **27**, 2464–2477.
91 H. Harashima, K. Sakata, K. Funato and H. Kiwada, *Pharm. Res.*, 1994, **11**, 402–406.

92 H. Harashima, H. Matsuo and H. Kiwada, *Adv. Drug Delivery Rev.*, 1998, **32**, 61–79.
93 J. S. Dordick, A. A. Vertegel and R. W. Siegel, *Langmuir*, 2004, **20**, 6800–6807.
94 W. Shang, J. H. Nuffer, V. A. Muñiz-Papandrea, W. Colón, R. W. Siegel and J. S. Dordick, *Small*, 2009, **5**, 470–476.
95 M. S. Ehrenberg, A. E. Friedman, J. N. Finkelstein, G. Oberdörster and J. L. McGrath, *Biomaterials*, 2009, **30**, 603–610.
96 M. J. D. Clift, S. Bhattacharjee, D. M. Brown and V. Stone, *Toxicol. Lett.*, 2010, **198**, 358–365.
97 G. Borchard and J. Kreuter, *Pharm. Res.*, 1996, **13**, 1055–1058.
98 O. Lunov, T. Syrovets, C. Loos, J. Beil, M. Delecher, K. Tron, G. U. Nienhaus, A. Musyanovych, V. Mailander, K. Landfester and T. Simmet, *ACS Nano*, 2011, **5**, 1657–1669.
99 J. T. P. Derksen, H. W. M. Morselt, D. Kalicharan, C. E. Hulstaert and G. L. Scherphof, *Exp. Cell Res.*, 1987, **168**, 105–115.
100 A. Beduneau, Z. Y. Ma, C. B. Grotepas, A. Kabanov, B. E. Rabinow, N. Gong, R. L. Mosley, H. Y. Dou, M. D. Boska and H. E. Gendelman, *PLoS One*, 2009, **4**, 2.
101 R. E. Serda, J. H. Go, R. C. Bhavane, X. W. Liu, C. Chiappini, P. Decuzzi and M. Ferrari, *Biomaterials*, 2009, **30**, 2440–2448.
102 D. Liu, Y. K. Song and F. Liu, *Pharm. Res.*, 1995, **12**, 1775–1780.
103 D. X. Liu, F. Liu and Y. K. Song, *Biochim. Biophys. Acta, Biomembr.*, 1995, **1235**, 140–146.
104 J. F. Scieszka, L. L. Maggiora, S. D. Wright and M. J. Cho, *Pharm. Res.*, 1991, **8**, 65–69.
105 S. M. Moghimi and A. C. Hunter, *Pharm. Res.*, 2001, **18**, 1–8.
106 V. K. Lishko, B. Kudryk, V. P. Yakubenko, V. C. Yee and T. P. Ugarova, *Biochemistry*, 2002, **41**, 12942–12951.
107 M. J. Hsu and R. L. Juliano, *Biochim. Biophys. Acta, Mol. Cell Res.*, 1982, **720**, 411–419.
108 S. M. Moghimi, A. C. Hunter and J. C. Murray, *Pharmacol. Rev.*, 2001, **53**, 283–318.
109 J. Kreuter, *Adv. Drug Delivery Rev.*, 2001, **47**, 65–81.
110 X. D. Yan, F. Kuipers, L. M. Havekes, R. Havinga, B. Dontje, K. Poelstra, G. L. Scherphof and J. A. A. M. Kamps, *Biochem. Biophys. Res. Commun.*, 2005, **330**, 1320–1320.
111 K. Nishikawa, H. Arai and K. Inoue, *J. Biol. Chem.*, 1990, **265**, 5226–5231.
112 G. A. Orr, W. B. Chrisler, K. J. Cassens, R. Tan, B. J. Tarasevich, L. M. Markillie, R. C. Zangar and B. D. Thrall, *Nanotoxicology*, 2011, **5**, 296–311.
113 S. Kanno, A. Furuyama and S. Hirano, *Toxicol. Sci.*, 2007, **97**, 398–406.
114 S. M. Moghimi, I. S. Muir, L. Illum, S. S. Davis and V. Kolbbachofen, *Biochim. Biophys. Acta, Mol. Cell Res.*, 1993, **1179**, 157–165.
115 K. D. Lee, R. E. Pitas and D. Papahadjopoulos, *Biochim. Biophys. Acta, Biomembr.*, 1992, **1111**, 1–6.
116 H. Matsuo, K. Funato, H. Harashima and H. Kiwada, *J. Drug Targeting*, 1994, **2**, 141–146.
117 H. Matsuo, C. Yamashita, K. Akiyama and H. Kiwada, *Biol. Pharm. Bull.*, 1995, **18**, 581–585.
118 A. Moore, R. Weissleder and A. Bogdanov, *J. Magn. Reson. Imaging*, 1997, **7**, 1140–1145.
119 S. M. Moghimi, C. J. H. Porter, I. S. Muir, L. Illum and S. S. Davis, *Biochem. Biophys. Res. Commun.*, 1991, **177**, 861–866.
120 W. H. De Jong, W. I. Hagens, P. Krystek, M. C. Burger, A. J. A. M. Sips and R. E. Geertsma, *Biomaterials*, 2008, **29**, 1912–1919.
121 P. Artursson, D. Johansson and I. Sjoholm, *Biomaterials*, 1988, **9**, 241–246.
122 A. Frana, P. Aggarwal, E. V. Barsov, S. V. Kozlov, M. A. Dobrovolskaia and A. Gonzalez-Fernandez, *Nanomedicine*, 2011, **6**, 1175–1188.
123 M. T. Peracchia, E. Fattal, D. Desmaële, M. Besnard, J. P. Noël, J. M. Gomis, M. Appel, J. d'Angelo and P. Couvreur, *J. Controlled Release*, 1999, **60**, 121–128.
124 I. Szleifer, *Biophys. J.*, 1997, **72**, 595–612.
125 J. Cheng, B. A. Teply, I. Sherifi, J. Sung, G. Luther, F. X. Gu, E. Levy-Nissenbaum, A. F. Radovic-Moreno, R. Langer and O. C. Farokhzad, *Biomaterials*, 2007, **28**, 869–876.
126 A. L. Klibanov, K. Maruyama, A. M. Beckerleg, V. P. Torchilin and L. Huang, *Biochim. Biophys. Acta, Biomembr.*, 1991, **1062**, 142–148.
127 R. Gref, M. Lück, P. Quellec, M. Marchand, E. Dellacherie, S. Harnisch, T. Blunk and R. H. Müller, *Colloids Surf., B*, 2000, **18**, 301–313.
128 A. Vonarbourg, C. Passirani, P. Saulnier and J. P. Benoit, *Biomaterials*, 2006, **27**, 4356–4373.
129 L. D. Unsworth, H. Sheardown and J. L. Brash, *Langmuir*, 2008, **24**, 1924–1929.
130 K. Knop, R. Hoogenboom, D. Fischer and U. S. Schubert, *Angew. Chem., Int. Ed.*, 2010, **49**, 6288–6308.
131 Y. Akiyama, T. Mori, Y. Katayama and T. Niidome, *J. Controlled Release*, 2009, **139**, 81–84.
132 S. D. Perrault, C. Walkey, T. Jennings, H. C. Fischer and W. C. W. Chan, *Nano Lett.*, 2009, **9**, 1909–1915.
133 K. Maruyama, *Adv. Drug Delivery Rev.*, 2011, **63**, 161–169.
134 F. Kawai, T. Kimura, M. Fukaya, Y. Tani, K. Ogata, T. Ueno and H. Fukami, *Appl. Environ. Microbiol.*, 1978, **35**, 679–684.
135 S. Stolnik, S. E. Dunn, M. C. Garnett, M. C. Davies, A. G. Coombes, D. C. Taylor, M. P. Irving, S. C. Purkiss, T. F. Tadros, S. S. Davis and L. Illum, *Pharm. Res.*, 1994, **11**, 1800–1808.
136 T. Tagami, Y. Uehara, N. Moriyoshi, T. Ishida and H. Kiwada, *J. Controlled Release*, 2011, **151**, 149–154.
137 R. Konradi, B. Pidhatika, A. Muhlebach and M. Textort, *Langmuir*, 2008, **24**, 613–616.
138 Z. G. Estephan, J. A. Jaber and J. B. Schlenoff, *Langmuir*, 2010, **26**, 16884–16889.
139 J. Ladd, Z. Zhang, S. Chen, J. C. Hower and S. Jiang, *Biomacromolecules*, 2008, **9**, 1357–1361.
140 L. Zhang, H. Xue, Z. Q. Cao, A. Keefe, J. N. Wang and S. Y. Jiang, *Biomaterials*, 2011, **32**, 4604–4608.
141 E. Muro, T. Pons, N. Lequeux, A. Fragola, N. Sanson, Z. Lenkei and B. Dubertret, *J. Am. Chem. Soc.*, 2010, **132**, 4556–4557.
142 Z. G. Estephan, P. S. Schlenoff and J. B. Schlenoff, *Langmuir*, 2011, **27**, 6794–6800.
143 S. D. Li and L. Huang, *J. Controlled Release*, 2010, **145**, 178–181.
144 C. H. J. Choi, C. A. Alabi, P. Webster and M. E. Davis, *Proc. Natl. Acad. Sci. U. S. A.*, 2010, **107**, 1235–1240.
145 Z. M. Qian, H. Li, H. Sun and K. Ho, *Pharmacol. Rev.*, 2002, **54**, 561–587.
146 R. H. Müller and C. M. Keck, *J. Nanosci. Nanotechnol.*, 2004, **4**, 471–483.
147 H. R. Kim, K. Andrieux, S. Gil, M. Taverna, H. Chacun, D. Desmaële, F. Taran, D. Georgin and P. Couvreur, *Biomacromolecules*, 2007, **8**, 793–799.
148 N. M. Griffin, J. Yu, F. Long, P. Oh, S. Shore, Y. Li, J. A. Koziol and J. E. Schnitzer, *Nat. Biotechnol.*, 2010, **28**, 83–89.
149 H. Zhou, Q. Mu, N. Gao, A. Liu, Y. Xing, S. Gao, Q. Zhang, G. Qu, Y. Chen, G. Liu, B. Zhang and B. Yan, *Nano Lett.*, 2008, **8**, 859–865.
150 B. Schwikowski, P. Uetz and S. Fields, *Nat. Biotechnol.*, 2000, **18**, 1257–1261.
151 H. Liu, L. Jin, S. B. S. Koh, I. Atanasov, S. Schein, L. Wu and Z. H. Zhou, *Science*, 2010, **329**, 1038–1043.
152 V. S. Reddy, S. K. Natchiar, P. L. Stewart and G. R. Nemerow, *Science*, 2010, **329**, 1071–1075.
153 X. R. Xia, N. A. Monteiro-Riviere and J. E. Riviere, *Nat. Nanotechnol.*, 2010, **5**, 671–675.
154 D. Labarre, C. Vauthier, C. Chauvierre, B. Petri, R. Müller and M. M. Chehimi, *Biomaterials*, 2005, **26**, 5075–5084.
155 M. Lück, K. F. Pistel, Y. X. Li, T. Blunk, R. H. Müller and T. Kissel, *J. Controlled Release*, 1998, **55**, 107–120.
156 S. Schmidt and R. H. Müller, *Int. J. Pharm.*, 2003, **254**, 3–5.
157 C. Olbrich, A. Gessner, W. Schröder, O. Kayser and R. H. Müller, *J. Controlled Release*, 2004, **96**, 425–435.
158 R. H. Müller, D. Rühl, M. Lück and B. R. Paulke, *Pharm. Res.*, 1997, **14**, 18–24.
159 H. R. Kim, K. Andrieux, C. Delomenie, H. Chacun, M. Appel, D. Desmaële, F. Taran, D. Georgin, P. Couvreur and M. Taverna, *Electrophoresis*, 2007, **28**, 2252–2261.
160 H. Weyhers, W. Mehnert and E. B. Souto, *Int. J. Mol. Med. Adv. Sci.*, 2005, **1**, 196–201.

161 M. Lück, B. R. Paulke, W. Schröder, T. Blunk and R. H. Müller, *J. Biomed. Mater. Res.*, 1998, **39**, 478–485.
162 M. T. Peracchia, S. Harnisch, H. Pinto-Alphandary, A. Gulik, J. C. Dedieu, D. Desmaële, J. D'Angelo, R. H. Müller and P. Couvreur, *Biomaterials*, 1999, **20**, 1269–1275.
163 T. M. Göppert and R. H. Müller, *Eur. J. Pharm. Biopharm.*, 2005, **60**, 361–372.
164 R. Shegokar, M. Jansch, K. K. Singh and R. H. Müller, *Nanomed.: Nanotechnol., Biol. Med.*, 2011, **7**, 333–340.
165 C. Lemarchand, R. Gref, C. Passirani, E. Garcion, B. Petri, R. H. Müller, D. Costantini and P. Couvreur, *Biomaterials*, 2006, **27**, 108–118.
166 A. L. Capriotti, G. Caracciolo, C. Cavaliere, C. Crescenzi, D. Pozzi and A. Laganà, *Anal. Bioanal. Chem.*, 2011, **401**, 1195–1202.
167 T. Blunk, D. F. Hochstrasser, J. C. Sanchez, B. W. Müller and R. H. Müller, *Electrophoresis*, 1993, **14**, 1382–1387.